

EFFECTS OF HYPERONS ON THE VIBRATIONS OF NEUTRON STARS

WILLIAM D. LANGER

*Inst. for Space Studies, Goddard Space Flight Center, NASA, New York, N.Y., and Yale University
New Haven, Conn., U.S.A.*

and

A. G. W. CAMERON

*Belfer Graduate School of Science, Yeshiva University New York, N.Y., and Inst. for Space Studies,
Goddard Space Flight Center, NASA New York, N.Y., U.S.A.*

(Received 24 March, 1969)

Abstract. We calculate the effects of hyperons and resonance particles on the vibrations of neutron stars. Vibrating neutron stars can store large amounts of energy in their vibrations; the interaction of the vibrations with the atmosphere would produce electromagnetic radiation. If any process damps out the vibrations rapidly on an astronomical time scale (~ 1000 years) then vibrating neutron stars are not likely to be found. Previous work indicates that radiation by a neutrino URCA process ($N+N \rightarrow P+N+e^{-}+\bar{\nu}_e$) does not rapidly damp many of the neutron star models. Some neutron stars are predicted to contain massive baryons; here we study thermal damping by nonequilibrium reactions involving these baryons.

During vibrations the thermodynamic equilibrium state is changed and particle reactions attempt to restore equilibrium. If the reaction rates per particle are very rapid or slow compared to the frequency of vibration the system follows almost the same pressure-volume curve through both parts of the gas cycle, and very little work is done. In the intermediate case, when reaction rates are comparable to the frequency, damping is rapid.

We find that the reaction rates for weak interactions such as $N+N \leftrightarrow P+\Sigma^{-}$ (the Σ^{-} is the first hyperon to appear with increasing density in degenerate neutron star matter) are of the right magnitude to cause rapid damping. If there is a hyperon region in the star then it cannot sustain vibrations. We also consider the much faster (and hence less important) process $N+N \leftrightarrow P+\Delta^{-}$.

1. Introduction

Cameron (1959) suggested that hyperons would be components of very dense matter. Subsequently, several people worked out the equation of state for a very dense gas (nuclear densities) of elementary particles assuming an independent particle model (Ambartsumyan and Saakyan, 1960). The next improvement was to introduce interaction potentials for the neutrons and protons. Tsuruta (1964) used such equations of state to investigate the structure of neutron star models. Additional theoretical support for the existence of neutron stars comes from work on supernovae (Arnett, 1966) in which the remnant has neutron star properties.

It has also been suggested that vibrating neutron stars could act as energy sources with the vibrations interacting with the atmosphere to produce the stars' observable spectrum (X-ray, optical). Cameron (1965) has suggested that much of the X-ray spectrum results from synchrotron or bremsstrahlung processes which arise in the

Astrophysics and Space Science 5 (1969) 213–253; © D. Reide! Publishing Company, Dordrecht - Holland

magnetosphere of a vibrating star. The large number of recently discovered X-ray sources has lent new interest to the vibrating neutron star problem.

Large amounts of energy can be stored in vibrations of the star. However, vibrations would raise and lower the Fermi levels of the constituents of the gas allowing various particle reactions, such as



to release the energy and damp the vibrations. If neutrino processes, gravitational radiation, or external shock waves do not dissipate the energy too rapidly (on the order of thousands of years), then the stars should be observable. Calculations (Hansen, 1966) indicated that for many cases stars could vibrate for thousands of years retaining an energy reservoir sufficient to provide the energy output measured for some X-ray sources.

The modern period of study of neutron star matter began with Ambartsumyan and Saakyan (1960). They constructed an equation of state for a degenerate gas composed of leptons, pions, neutrons, protons and the low lying hyperons based on an independent particle model.

The next improvement to the model was to introduce an interaction potential for the neutrons and protons. Tsuruta (1964) used the V_{β} and V_{γ} potentials of Levinger and Simmons (1961) to write a better equation of state near and above nuclear densities. With the equation of state Tsuruta integrated the relativistic hydrostatic equations to obtain stellar models, and in this way determined which models gave stable neutron stars. Here we will extend the study of the neutron star properties by including the effects of some hyperon reactions on the damping of vibrations.

Bahcall and Wolf (1965) studied neutrino producing reactions, such as Equation (1), to determine how long it would take a neutron star to cool down to temperatures at which the surface would emit X-rays too soft for observation. Hansen (1966) and Hansen and Tsuruta (1967) studied these reactions for the general case of a vibrating neutron star with thermal feedback from the reactions. And, as previously mentioned, their conclusion was that vibrating neutron stars could not be ruled out as energy storage sources for X-ray emission. Some models vibrated long enough, and could store enough energy, to correspond to the energy output of some present day X-ray sources.

In the independent particle model the hyperons begin to appear in significant numbers when there is sufficient energy to create them. Each hyperon appears at a different threshold value of the neutron number density and the first to appear is the Σ^{-} . Next follows the Λ^0 and then the first resonance particle, the Δ^{-} (also called $N_{3/2}^*$ (1236)).

There are numerous reactions which produce the various hyperons and resonances, and, without some physical insight, the task of investigating them would be formidable. The physics behind our choice lies in a knowledge of the interaction coupling constants, and a more subtle understanding of the role of phase space in a degenerate gas.

In a degenerate Fermi gas the lowest lying states are filled up and if a particle is

produced it must have sufficient energy to occupy one of the unfilled states. The particle which participate in the reactions come from the top of the Fermi sea; very few particles will be above the Fermi level. A strangeness conserving strong interaction, such as



is strongly inhibited because the nucleons must have enough energy to create a K^+ rest mass ~ 494 MeV plus the energy difference between $P + \Sigma^-$ and the two N 's. In a neutron star $E_F(N)$ (the total neutron Fermi energy) is typically $\sim 10^3$ MeV, the number of neutrons with sufficient energy (i.e. ~ 1400 MeV) for the reaction is proportional to $e^{-(E-E_F(N))/kT}$ (from the Fermi distribution), and is an insignificant number (here we consider $T < 10^{10}$ K).

Similar problems occur for reactions such as



because momentum conservation requires large $E(e^-)$, which are $\gg E_F(e^-)$. We soon learn to look for weak interactions, which do not have to produce particles such as K mesons, because they violate strangeness. In addition, the reactions should involve massive baryons so that energy and momentum conservation can be satisfied with the Fermi level values (available states at the top of the Fermi sea). From these considerations the first reaction important for the damping process is,



which is predicted, and can be studied, from the coupling of the hadronic terms of Cabibbo's (1963) vector-axial vector currents in weak interactions (similarly for the other weak hyperon interactions). Reaction rates for the resonances, such as the Δ^- (the next particle to appear after the Σ^-), can be studied in strong interactions with a modified one pion exchange.

Under non-vibrational conditions the forward and reverse rates for a reaction keep the particles in equilibrium. When the star vibrates, the reaction rates will go out of equilibrium (for a discussion of equilibrium see Tsuruta and Cameron, 1966) and it becomes possible to transfer vibrational energy into thermal energy.

To understand why the reactions are no longer in equilibrium, let us look at what the vibrations do to the dense matter. In a degenerate gas the Fermi momentum $P(F)$ is

$$P_i(F) \propto N_i^{1/3}, \quad (5)$$

where N_i is the number density for particle i , and the Fermi energy is

$$E_i(F) = [P_i^2(F) C^2 + M_i^2 C^4]^{1/2}. \quad (6)$$

When the system is vibrating the number densities change; hence the Fermi momentum and energy change, but not such that the sum of the in and out Fermi energies for a reaction are equal (i.e. if $E_F(N) = E_F(P) + E_F(e^-)$ the neutrons, protons and electrons are in equilibrium with each other). With the forward and reverse rates unequal,

the reactions proceed to restore equilibrium, and in the process vibrational energy can be transferred to thermal energy.

To find the amount of energy lost through damping we calculate the work that a volume of gas does in a cycle. If we study a PV diagram during a cycle we can evaluate how much work is done on the gas. In this way we can measure the rate at which vibrational (mechanical) energy is converted to thermal (heat) energy.

For no reactions the system stays in equilibrium and no work is done (providing $T = \text{constant}$). When the reaction rates are very low compared to the vibrational frequency the system never deviates much from equilibrium and there is very little work done per cycle. For very fast rates (orders of magnitude faster than the vibrational frequency) the system effectively stays in equilibrium and again very little work is done. This case is like that of an adiabatic system. In the intermediate case damping is rapid, here there is a large difference between the equilibrium state and the actual state.

In this work we found that where the neutron stars had cores dense enough to contain hyperons, there are reactions which can rapidly damp vibrations. The non-equilibrium rates for reactions like (4) are, for large amplitudes of vibration, comparable to the vibrational frequency. Hence rapid damping occurs in the core, and only very small amplitudes can survive for periods of time long on an astronomical time scale; small amplitude oscillations cannot store meaningful amounts of energy.

Very fast reactions, such as



proceed via a strong interaction, and can occur at the top of the Fermi sea. These reactions are so fast as to restore equilibrium (with respect to these particles) throughout the cycle, and do not affect damping.

2. Reaction Rates

A. INTRODUCTION

Before calculating any reaction rates we will outline some results of quantum field theory (QFT). Many excellent texts develop this subject in detail; here we present only the results which will be of use in this paper.

When we solve the Schrodinger equation in quantum mechanics, $H \neq H(t)$ and

$$i \frac{\partial \Psi(t)}{\partial t} = H \Psi(t). \quad (8)$$

In QFT we work in the interaction representation where both H and Ψ are functions of t . Here we satisfy the equation

$$i \frac{\partial \Psi(t)}{\partial t} = H(t) \Psi(t) \quad (9)$$

with a solution of the form

$$\Psi(t_1) = U(t_1, t_0) \Psi(t_0). \quad (10)$$

Equation 9 can be solved by an iterative procedure, so that

$$U(t, t_0) = \sum_0^{\infty} \frac{(-i)^n}{n!} \int_{t_0}^t dt_1 \cdots \int_{t_0}^t dt_n T(H(t_1) \cdots H(t_n)), \quad (11)$$

where T is the time ordering operator and has the following property

$$T\{H(t_1) H(t_2)\} = H(t_1) H(t_2) \Theta(t_1 - t_2) + H(t_2) H(t_1) \Theta(t_2 - t_1) \quad (12)$$

and θ is a step function. In this picture H can be written as a free plus interaction term

$$H = H_{\text{free}} + H_{\text{int}}. \quad (13)$$

Now

$$U(t, t_0) = T\left\{\exp\left[-i \int_{t_0}^t \mathcal{H}_{\text{int}}(\varphi_I, \Psi_I) d^4x\right]\right\}, \quad (14)$$

where \mathcal{H} is a hamiltonian density, and the φ_I and ψ_I are boson and fermion wave function solutions to a free equation with

$$\varphi_I(t, \mathbf{x}) e^{iH_0 t} \varphi_{\text{Sch}}(\mathbf{x}) e^{-iH_0 t}. \quad (15)$$

From U one defines the scattering operator

$$S = U(\infty, -\infty) = T\left\{\exp\left[-i \int \mathcal{H}_{\text{int}} d^4x\right]\right\} \quad (16)$$

with the integral extending over all four space.

If it does not contain derivative couplings S is a Lorentz invariant. S is evaluated between states which are free particles at $t \rightarrow \pm \infty$, ($|\alpha(-\infty)\rangle_I$ = incoming state and $|\alpha(\infty)\rangle_I$ = outgoing state). The terms $\langle \alpha | S | \beta \rangle$ will contain only free fields; this points out the obvious advantage of the S matrix approach, that of working with free fields.

There is a connection between this S matrix formulation and Feynman diagrams. Each order in the expansion of Equation (16) generates sets of terms which can be interpreted as Feynman diagrams. Before developing this approach we must discuss normal products, propagators and Wick's theorem.

A normal product of operators in QFT, denoted as: $AB\dots$, is a product of annihilation and creation operators in which all annihilation operators are placed to the right of all creation operators. Thus the expectation of the normal product between vacuum states is zero.

Consider φ_1 and φ_2 , two Hermitian fields which are independent but create and destroy particles with the same mass. From them we can construct nonhermitian linear combinations with the properties:

- $\varphi^{(+)}(x)$ annihilates a particle
- $(\varphi^{(+)}(x))^\dagger$ creates a particle
- $\varphi^{(-)}(x)$ creates an antiparticle
- $(\varphi^{(-)}(x))^\dagger$ annihilates an antiparticle.

So terms like $\langle 0 | \varphi(x) \varphi^\dagger(y) | 0 \rangle$ will appear but not $\langle 0 | \varphi(x) \varphi(Y) | 0 \rangle$ (φ a sum of $\varphi^{(+)}$ and $\varphi^{(-)}$ annihilates on the vacuum). We can interpret surviving terms, such as, $\langle 0 | \varphi^{(+)}(x) (\varphi^{(-)}(y))^\dagger | 0 \rangle$ as a particle created as a spacetime point y , propagating to x where it is annihilated.

This suggests a graphical technique. If time flows from left to right $\cdot \rightarrow = (\varphi^{(+)}(x))^\dagger | 0 \rangle$ and $\rightarrow \cdot = \langle 0 | \varphi^{(+)}(y)$. It was Feynman who identified an antiparticle travelling forward in time with a negative energy particle travelling backwards in time.

Now our propagators also are solutions of a Green's function equation

$$\Delta_F(x - y) = i \langle 0 | T \{ \varphi(x) \varphi^\dagger(y) \} | 0 \rangle \tag{17}$$

is a Green's function solution to

$$\left(\frac{\partial}{\partial x_\lambda} \frac{\partial}{\partial x_\lambda} - \mu^2 \right) \Delta_F(x - x^1) = - \delta(x - x^1), \tag{18}$$

where μ is the mass of the particle and F refers to the Feynman contour. If we Fourier transform to work with $G(k)$ this contour in the k^0 plane is shown in Figure 1a (it is usually simpler to solve for $G(k)$).

If $x^0 > y^0$ $\Delta_F(x - y)$ represents a particle created at (y^0, \mathbf{y}) and travelling forward in time to (x^0, \mathbf{x}) where it is annihilated. If $y^0 > x^0$ it represents an antiparticle created at (x^0, \mathbf{x}) and travelling forward in time to (y^0, \mathbf{y}) where it is annihilated (see Figure 1b).

Δ_F is also called a contraction, and this notation appears in the last point in our

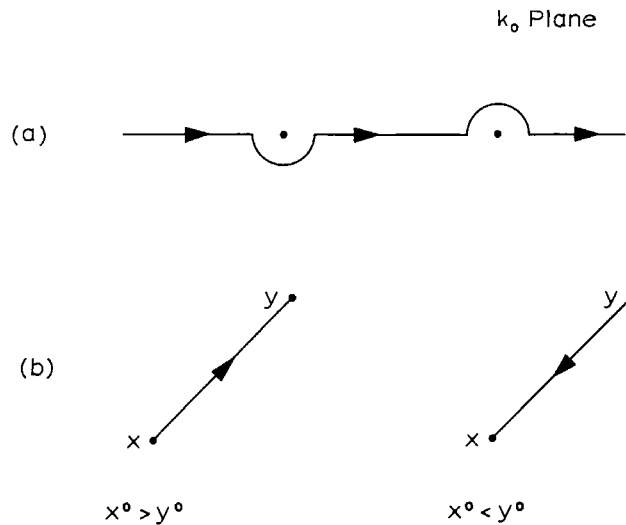


Fig. 1. (a) Green's function contour in the k plane. – (b) Schematic representation for the Green's function.

digression, Wick's theorem. Wick's theorem rewrites a time ordered product as a sum of normal ordered terms and contractions as follows:

$$\begin{aligned}
 T\{\varphi(1)\varphi(2)\dots\varphi(n)\} &=:\varphi(1)\dots\varphi(n): \\
 &+ \langle 0|T(\varphi(1)\varphi(2))|0\rangle:\varphi(3)\dots\varphi(n): \\
 &+ \text{all permutations of one contraction} \\
 &+ \sum(\text{all permutations of two contractions}) \\
 &+ \dots \\
 &+ \sum \begin{cases} \text{(all permutations of } N/2 \text{ contractions (} N \text{ even))} \\ \text{(all permutations of } ((N-1)/2) \text{ contractions (} N \text{ odd))} \end{cases}. \quad (19)
 \end{aligned}$$

Now the vacuum expectation value of a normal product vanishes so that for n even

$$\begin{aligned}
 \langle 0|T(\varphi(1)\dots\varphi(n))|0\rangle \\
 = \sum \delta_p \langle 0|T(\varphi(1)\varphi(2))|0\rangle \dots \langle 0|T(\varphi(N-1)\varphi(N))|0\rangle \quad (20)
 \end{aligned}$$

where the sum is over all the permutations and δ_p is the sign of the permutation of the Fermi fields (each permutation for a Fermi field introduces $a-1$). For n odd the vacuum expectation value is zero. We will now be able to express the S matrix in terms of the Feynman propagators for free particles using their physical masses.

There are other contractions for the Dirac and electromagnetic field, for the Dirac field it is

$$\begin{aligned}
 \langle 0|T(\psi_\alpha(x)\psi_\beta(y))|0\rangle &= iS_F(x-y, m)_{\alpha\beta} \\
 &= i \int \frac{d^4p}{(2\pi)^4} \frac{e^{-ip \cdot (x-y)}(\not{p} + m)}{p^2 - m^2 + i\epsilon}. \quad (21)
 \end{aligned}$$

In the expansion of the S matrix some terms correspond to renormalization and some to vacuum bubbles. We will not, within this limited review, discuss these in detail; an example should clarify what we have done.

Consider the interaction of two charged fermion fields with a noncharged scalar boson field

$$\mathcal{H}_{\text{int}}(x) = g\Psi^\dagger(x)\Psi(x)\varphi(x). \quad (22)$$

In the second order we have (the first order term is zero between the vacuum states)

$$\begin{aligned}
 S^{(2)} &= g^2 \frac{(-i)^2}{2!} \int d^4x_1 d^4x_2 T\{:\Psi^\dagger(x_1)\Psi(x_1)\varphi(x_1): \\
 &\times :\Psi^\dagger(x_2)\Psi(x_2)\varphi(x_2):\}. \quad (23)
 \end{aligned}$$

There are nine terms generated by the T operator, we will look at four of these

$$=:\Psi^\dagger(x_1)\Psi(x_1)\varphi(x_1)\Psi^\dagger(x_2)\Psi(x_2)\varphi(x_2): \quad (24a)$$

$$+:\Psi(x_1)\varphi(x_1)\Psi^\dagger(x_2)\varphi(x_2):S_F(1-2) \quad (24b)$$

$$+ : \Psi^\dagger(x_1) \Psi(x_2) : S_F(2-1) \Delta_F(2-1) \tag{24c}$$

$$+ \Delta_F(2-1) S_F(2-1) S_F(2-1) + \dots \tag{24d}$$

The Feynman diagrams for these terms are shown in Figure 2a-d. As in $S^{(1)}$ the vacuum expectation of disconnected graphs like Figure 2a (Equation 24a) is zero. Figure 2b is called a Compton graph and corresponds to a scattering process. Figure 2c is called a self energy diagram and it changes the mass of a particle. It is interpreted that part of the time a charged particle is a superposition of a charged particle and a neutral particle. The change in the mass from self energy diagrams is infinite; when we can add a finite number of infinite mass counter terms to H_{int} to cancel the self energy infinities and leave a finite observable, the theory is renormalizable. Figure 2d is a vacuum fluctuation and only affects the phase of S .

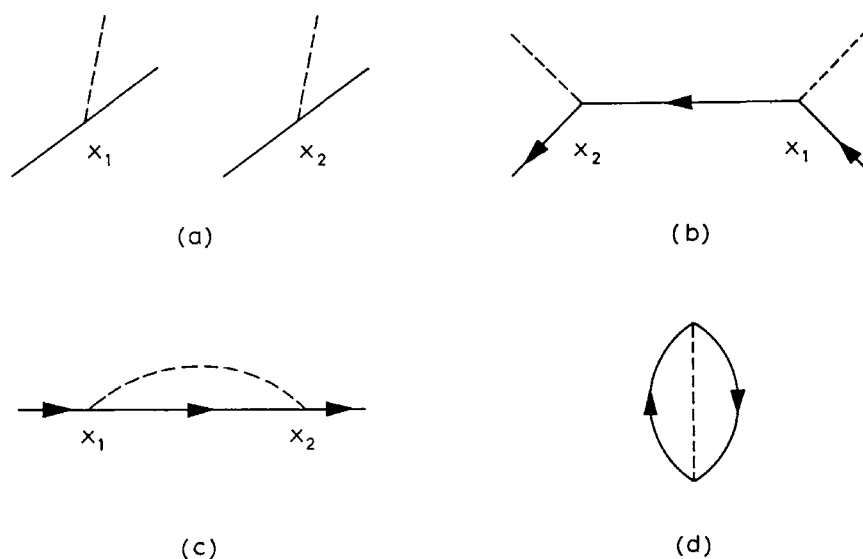


Fig. 2. Some Feynman diagrams for the second order term of a noncharged scalar field interacting with two charged fermion fields.

For the S matrix expansion to have a meaning $g \ll 1$ and it must be renormalizable; these conditions hold for quantum electrodynamics. In strong interactions $g \simeq 15$; in weak interactions $g \ll 1$, but the theories constructed are not renormalizable (however we will see that this type of theory will give excellent results at low energies).

In the weak interactions we will have a product of four ψ 's as well as γ matrices. We take the ψ 's as plane waves in the following form

$$\Psi_i(x) = \sqrt{\frac{m_i}{E_i V}} u(p_i, S_i) e^{-ip_i \cdot x}, \tag{25}$$

where ψ has been normalized in a box of volume V , m is the mass, E the energy and u the spinor (a function of momentum p and spin s) of particle i . When $\bar{\psi}_1 O \bar{\psi}_2 \psi_3 O' \psi_4$

(where O is an operator) is put into S and we integrate over d^4x we get

$$S^{(1)} = -\frac{i(2\pi)^4}{V^2} \delta^4(p_1 + p_3 - p_2 - p_4) \left[\prod_{j=1}^4 \frac{m_j}{E_j} \right]^{1/2} \times \{ \bar{u}(1) O u(2) \bar{u}(3) O' u(4) \} \quad (26)$$

denoting $\{ \}$ by $M^{(1)}$ (see Figure 3 for the $S^{(1)}$ Feynman diagram).

In general, in momentum space we can write S as

$$S_{fi} = \delta_{fi} - (2\pi)^4 \delta^4(p_f - p_i) \left[\prod_{j=1}^4 \frac{m_j}{E_j} \right]^{1/2} M_{fi}, \quad (27)$$

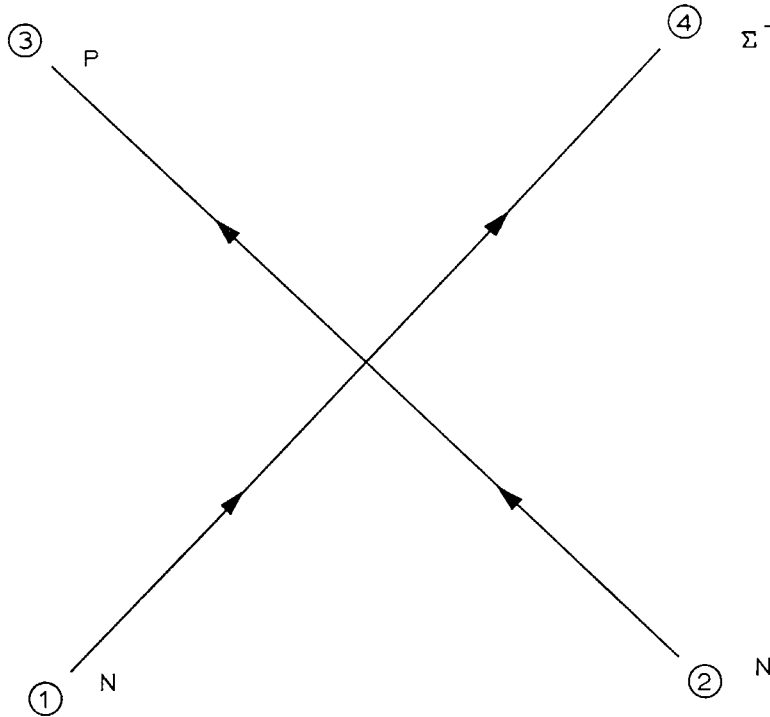


Fig. 3. Feynman diagram for the first order interaction of the coupled weak hadronic currents for the reaction $N+N \rightarrow P+\Sigma^-$.

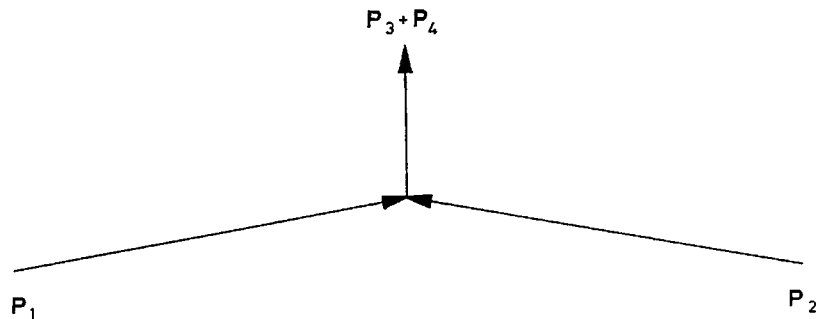


Fig. 4. A momentum diagram for $N+N \rightarrow P+\Sigma^-$ where the momentum values are taken at the top of the fermi sea. 1 and 2 are the neutrons, 3 the proton and 4 the Σ^- .

where f, i refer to the final and initial states respectively, and M_{fi} is the transition matrix. Here we have set $V=1$ as V does not appear in the final results of the observables which are measured (cross sections, etc.) Following Bjorken and Drell (1964) we can derive the transition rate W_{fi} unit volume

$$W_{fi} = \frac{|S_{fi}|^2}{T} = (2\pi^4) \delta^4(p_f - p_i) \prod_{j=1}^4 \frac{m_j}{E_j} |M|^2, \quad (28)$$

where we have used

$$[(2\pi)^4 \delta^4(p_f - p_i)]^2 \rightarrow T(2\pi)^4 \delta^4(p_f - p_i) \quad (29)$$

and take the limit of the observation time T going to infinity.

The physics in the problem is located in $|M|^2$. $|M|^2$ is a product of spinors which we will sum over final states and average over initial states; for this procedure we will need the energy projection operators

$$\sum_{S_i} u_\beta(p_i, S_i) \bar{u}_\lambda(p_i, S_i) = \left(\frac{\not{p}_i + m_i}{2m_i} \right)_{\beta\lambda}, \quad (30)$$

where we use the Feynman slash notation $\not{f} = \gamma_\mu f^\mu$. $|M|^2$ will reduce to a trace (or product of traces) and can be evaluated through the trace theorems (Bjorken and Drell, 1964).

Using Equation (28) and summing over the available phase space we have the reaction rate per unit volume

$$\begin{aligned} \frac{dn}{dt} = & \int \cdots \int S(p_1) S(p_2) (1 - S(p_3)) (1 - S(p_4)) \\ & \times (2\pi)^4 \delta^4(p_f - p_i) |M|^2 \frac{1}{(2\pi)^{12}} \prod_{j=1}^4 \frac{m_j}{E_j} d^3 p_j, \end{aligned} \quad (31)$$

where $S(P)$ is the Fermi distribution function

$$S(p) = [1 + \exp(\beta(E - E(F)))]^{-1} \quad (32)$$

(the Fermi distribution must be used because the reactions occur in a degenerate gas) and $\beta=1/kT$, k is Boltzmann's constant, T is the temperature in degrees Kelvin and $E(F)$ is the Fermi energy. $S(P)$ represents the available states for the initial particles (occupied states), while $(1 - S(P))$ represents the unoccupied states available to the final particles. For the inverse reaction we need only replace the Fermi phase space factors by

$$S(p_3) S(p_4) (1 - S(p_2)) (1 - S(p_1)) \quad (33)$$

as $|M|^2$ is an invariant quantity. $|M|^2$ does not vary much over a small region of phase space, it can thus be taken out of the integral for a situation where, as will

later be shown to be the case for the reactions considered here, only a small part of phase space contributes to the reactions.

Specifically the reaction



will be discussed, but much of what is said can be applied to other reactions of interest.

We write Equation (31) as

$$\frac{dn}{dt} = |M|^2 P, \quad (35)$$

where

$$P = \frac{1}{(2\pi)^8} \int \cdots \int S(p_1) S(p_2) (1 - S(p_3)) (1 - S(p_4)) \\ \times \delta^4(p_1 + p_2 - p_3 - p_4) \prod_{j=1}^4 \frac{m_j}{E_j} d^3 p_j. \quad (36)$$

B. PHASE SPACE

In evaluating the phase space part of dn/dt we can make use of some simplifications. Most of the reactions involve particles from a narrow band at the top of the Fermi sea. In the region of interest the neutron Fermi momentum is greater than that of either the proton or sigma minus (typically $P_F(n) \sim 5 \times 10^2$ MeV/c, $P_F(P)$ and $P_F(\Sigma^-) \sim 1.5 \times 10^2$ MeV/c), momentum conservation is shown in Figure 4, where 1 and 2 are the neutrons, 3 the proton and 4 the sigma minus momenta.

Conservation of energy and momentum, and the distribution factors $S(P)$, restrict most of the reactions to a small part of phase space and greatly simplify the calculation (Bahcall and Wolf, 1965, and Hansen, 1966). It should be noted that in these calculations $\hbar = c = 1$, and in the final results we evaluate in the appropriate units. Rewriting P

$$P = \frac{1}{(2\pi)^8} \int \cdots \int \delta(E_f - E_i) S(p_1) S(p_2) (1 - S(p_3)) (1 - S(p_4)) \\ \times \prod_{j=1}^4 \frac{m_j}{E_j} p_j^2 dp_j A, \quad (37)$$

where

$$A = \int \delta^3(\mathbf{p}_f - \mathbf{p}_i) \prod_{j=2}^4 d\Omega_j. \quad (38)$$

Equation 38 can be evaluated to yield

$$A = \frac{(4\pi)^3}{2 |\mathbf{p}_1| |\mathbf{p}_2| |\mathbf{p}_3|}, \quad (39)$$

where we have used the momentum condition in a neutron star $0 < |\mathbf{P}_p + \mathbf{P}_{\Sigma^-}| < 2|\mathbf{P}_N|$.

Substituting Equation (39) into Equation (37), using $p dp = E dE$ and then canceling with $\pi_j 1/E_j$ we have

$$p \frac{4}{(2\pi)^5} \int \cdots \int S(p_1) S(p_2) (1 - S(p_3)) (1 - S(p_4)) \times \delta(E_f - E_i) p_4 \prod_{j=1}^4 m_j dE_j. \quad (40)$$

Now,

$$(1 - S(p)) = [1 + e^{-\beta(E - E(F))}]^{-1} \quad (41)$$

and this suggests a change variables. Setting

$$\begin{aligned} x_1 &= \beta(E_1 - E_1(F)), \\ x_2 &= \beta(E_2 - E_2(F)), \\ x_3 &= -\beta(E_3 - E_3(F)), \\ x_4 &= -\beta(E_4 - E_4(F)), \end{aligned} \quad (42)$$

and

$$\begin{aligned} P + \Sigma^- &\rightarrow N + N, \\ 3 + 4 &\rightarrow 1 + 2, \end{aligned} \quad (43)$$

for the reverse reaction we let $x_i \rightarrow -x_i$.

Using the substitution (42), integrating over dx_4 and using the delta function we have,

$$P = \frac{4}{(2\pi)^5} \frac{1}{\beta^4} \int_{-\infty}^{\infty} dx_1 \int_{-\infty}^{\infty} dx_3 \int_{-(x_1+x_3+\Delta)}^{\infty} dx_2 \left[1 + e^{-\left(\sum_i x_i + \Delta\right)} \right] \times \left[\left(\sum_1^3 x_i + \delta \right)^2 - \beta^2 m_4^2 \right]^{1/2} \prod_1^3 (1 + e^{x_i})^{-1}, \quad (44)$$

where

$$\Delta = \beta(E_1(F) + E_2(F) - E_3(F) - E_4(F))$$

and

$$\delta = \beta(E_1(F) + E_2(F) - E_3(F)).$$

The inverse reaction's equation has the same form but with Δ replaced by $-\Delta$. At equilibrium $\Delta = 0$ and the forward and inverse rates are equal.

As $M_3 \ll E_3(F)$ the limit on X_3 can be extended to $+\infty$ with very little error. In the E integrations we have $\int_{m_1}^{\infty} dE_1 \int_{E_3+m_4-E_1}^{\infty}$ in our calculations we can set $E_4(F) \approx M_4$. In E_1 we can replace M_1 by $-\infty$ and the lower limit in $\int dE_2$ comes from $E_1 + E_2 \geq E_3 + M_4$. In the x_i representation

$$x_2|_{\min} = \beta(E_2 - E_2(F))|_{\min} = -(x_1 + x_3 + \Delta). \quad (45)$$

Equation 44 can be reduced to a single dimensionless integral $I(\Delta)$. This solution is straightforward, but tedious, and is relegated to Appendix A. The result is

$$I(\Delta) = \int_{-\Delta}^{\infty} [(y + \delta)^2 - \beta^2 m_4^2]^{1/2} (3\zeta(2) + \frac{1}{2}y^2) \times (1 + e^y)^{-1} (1 + e^{-(y+\Delta)})^{-1} dy, \quad (46)$$

where ζ is the Reimann zeta function, y a dummy variable, and now

$$P \frac{4I(\Delta)}{(2\pi)^5 \beta^4}. \quad (47)$$

The evaluation of phase space for a four particle reaction (two in, two out) of fermions in a degenerate gas is applicable to any of the reactions that we are interested in, and is quite general as to forward or reverse reactions.

C. TRANSITION MATRIX FOR $N + N \rightarrow P + \Sigma^-$

The theory which has met with the most success for weak interactions is based on constructing an interaction Hamiltonian from currents

$$H_{\text{int}} = \frac{G}{2\sqrt{2}} [j_\lambda j^{\lambda\dagger} + j_\lambda^\dagger j^\lambda]. \quad (48)$$

This interaction is an extrapolation from quantum electrodynamics (QED), but unlike QED the currents are not coupled to a field associated with a propagator. The currents, like those in QED, are binomial in the ψ 's, so that H_{int} is a product of four fermion wave functions. In the lowest order this represents four fermions interacting at a point with G , the coupling constant, a measure of the strength of the interaction (as α does for QED). It would seem that since G , like α , is $\ll 1$, the perturbation expansion of Section 2-A would be valid. However, a point interaction with four fermion lines in the first order perturbation violates unitarity (i.e. the probability for a transition exceeds one) at high energies (hundreds of GeV). Yet phenomenologically this interaction in the first order perturbation provides excellent agreement with experiment at relatively low energies.

Historically, the near equality of the experimentally determined coupling constants in beta decay, involving hadronic and leptonic elements, and muon decay, a purely leptonic interaction, suggested that a universal coupling existed for weak interactions. The adjoint leptonic (L) current is

$$j_\lambda^{L\dagger} = \bar{\psi}_e \gamma_\lambda (1 - \gamma_5) \psi_{\nu_e} + \bar{\psi}_\mu \gamma_\lambda (1 - \gamma_5) \psi_{\nu_\mu}. \quad (49)$$

The $\gamma_\lambda \gamma_5$ term, not found in QED, generates an axial vector current which violates parity, quite admissible in weak interactions which are known to violate parity. The sign in front of the γ_5 is different in the various texts, and depends on the authors

definition of γ_5 ; here we use $\gamma_5 = \begin{pmatrix} 0 & 1 \\ 1 & 0 \end{pmatrix}$. The hadronic (H) current for beta decay is

$$j_\lambda^H = \bar{\psi}_p \gamma_\lambda (1 - r\gamma_5) \psi_n. \quad (50)$$

The factor r represents the effects of the strong interactions on the axial vector part of the current. The explanation of why this occurs was provided by Feynman and Gell-Mann (1958) and independently by Gershtein and Zeldovich (1955). They pointed out that a similar effect occurs in QED; an electron and a proton have the same charge despite the presence of the pion interaction of the proton, this is a direct result of the conservation of electromagnetic current. For example a proton emitting a neutron and π^+ conserves charge. That is, the strong interactions, which conserve charge, will not affect the electromagnetic interaction. Said in another way, A_μ , the vector potential, will couple with the conserved charge current which is the sum of the proton and π^+ currents.

The weak interaction current $j_\lambda^{V(H)}$ changes charge by one and it can be related to I^+ the isospin raising operator (which also changes charge by one). Feynman and Gell-Mann's hypothesis was that $j_\lambda^{V(H)}$ is also a conserved vector current (CVC), and I^+ is the weak interaction conserved quantity corresponding to the conservation of charge in electrodynamics (which corresponds to I_3). The close relationship between these two currents is also emphasized by noting that the part of $j^{EM} \propto I_3$ will be related to $j_\lambda^{V(H)}$ by a rotation in isotopic (I) spin space.

The axial vector current is not a conserved quantity (much attention has been focused on the concept of a partially conserved axial current, PCAC, where the divergence of the current is proportional to the pion current) and hence the pions will renormalize the strength of the interaction relative to the vector current.

We would now write the total current as

$$j_\lambda = j_\lambda^{(H)} + j_\lambda^{(L)}. \quad (51)$$

The coupling of the currents would give the various weak interaction processes, i.e. neutron (beta) decay, electron and muon capture, etc.

The currents as we have written them suffice for reactions which involve the small momentum transfers typical of beta decay; at higher momentum transfers form factors become important (Brene *et al.*, 1964). The CVC postulate links the weak interactions to the electromagnetic and the electromagnetic interactions require form factors. These form factors represent the deviation of the actual particle from a point source (Wu, 1964). Experimentally it was found that a straightforward extending of the above concepts to the hyperons gave results often off by orders of magnitude. A successful extension of this technique to strange particles is due to Cabibbo (1963) and is based on $SU(3)$. The hadronic current is now written in terms of a strangeness conserving ($\Delta S=0$) and a strangeness violating ($|\Delta S|=1$) term coupled universally

$$j_\lambda^H = \cos \Theta j_\lambda^{(0)} + \sin \Theta j_\lambda^{(1)}. \quad (52)$$

Cabibbo's model also contains the following assumptions:

1) The total current j behaves as a sum of octet members under $SU(3)$ transformations. We can use the members of the pseudoscalar meson octet to illustrate the transformation properties, so that: $j^{(0)}$ transforms like a charged pion with strangeness zero, and $j^{(1)}$ will transform like the K^+ which is the only $S=1$ meson in the pseudoscalar octet (a review of the $SU(3)$ structure and properties is in Appendix B):

2) Assuming the conserved vector current (CVC) hypothesis, $j^{v(0)}$ is proportional to the isospin current $I^{(+)}$. This assumption can be extended, and it is assumed $j^{v(0)}$ and $j^{v(1)}$ are proportional to an octet of currents containing $I^{(+)}$:

3) No symmetry breaking is included and $SU(3)$ is held to be exact.

The matrix elements are written as

$$\langle \bar{B} | j^{(0)} | B \rangle \quad \text{and} \quad \langle \bar{B} | j^{(1)} | B \rangle$$

where B and \bar{B} represent the baryon states. From the results in Appendix B for D and F -type couplings which correspond to π^+ transformations for $j^{(0)}$ and K^+ for $j^{(1)}$, we have four couplings

$$\begin{aligned} \text{a)} \quad D^{(0)} &= \bar{P}n + \bar{\Sigma}^0 \Sigma^- + \sqrt{\frac{2}{3}} \bar{\Sigma}^+ \Lambda + \sqrt{\frac{2}{3}} \bar{\Lambda} \Sigma^-, \\ \text{b)} \quad F^{(0)} &= \bar{P}n - \bar{\Sigma}^0 \Sigma^- - \sqrt{2} \bar{\Sigma}^+ \Sigma^0 + \sqrt{2} \bar{\Sigma}^0 \Sigma^-, \\ \text{c)} \quad D^{(1)} &= \bar{P} \left(\frac{1}{\sqrt{2}} \Sigma^0 - \frac{1}{\sqrt{6}} \Lambda \right) + \left(\frac{1}{\sqrt{2}} \bar{\Sigma}^0 - \frac{1}{\sqrt{6}} \bar{\Lambda} \right) \Sigma^- + \bar{n} \Sigma^- + \bar{\Sigma}^+ \Sigma^0, \\ \text{d)} \quad F^{(1)} &= -\bar{P} \left(\frac{1}{\sqrt{2}} \Sigma^0 + \sqrt{\frac{3}{2}} \Lambda \right) + \left(\frac{1}{\sqrt{2}} \bar{\Sigma}^0 + \sqrt{\frac{3}{2}} \bar{\Lambda} \right) \Sigma^- - \bar{n} \Sigma^- + \bar{\Sigma}^+ \Sigma^0. \end{aligned} \quad (53)$$

Now $D^{(0)}$ can be discarded because terms like $\bar{\Sigma}^+ \Lambda$ are not matrix elements of $I^{(+)}$. The strength of the $F^{(0)}$ coupling in j_λ^v is determined by letting $\bar{P}n$ represent the Fermi transitions in beta decay (hence the coupling is unity). From experiments on hyperon decays the three unknown parameters θ , f_A and d_A can be determined, where f_A and d_A are the F and D coupling strengths for the axial vector coupling (the set of values used here, Frazer 1966, are $\theta = 0.254$ radians, $f_A = 0.437$ and $d_A = 0.742$).

We now write

$$\langle \bar{B} | j_\lambda^H | B \rangle = \cos \theta \langle \bar{B} | j_\lambda^{(0)} | B \rangle + \sin \theta \langle \bar{B} | j_\lambda^{(1)} | B \rangle, \quad (54)$$

where

$$\langle \bar{B} | j_\lambda^{(1)} | B \rangle = \gamma_\mu \gamma_5 [d_A D_{\bar{B}B}^{(i)} + f_A F_{\bar{B}B}^{(i)}] + \gamma_\mu F_{\bar{B}B}^{(i)} \quad (55)$$

and $i=0,1$.

For the reactions of interest in this work, the momentum transfers are larger than those involved in ordinary beta decay, and form factors are needed for each vertex (Brene, *et al.*, 1964). Following BHR we introduce an $F(q^2)$ where $q^2 = (P_{\bar{B}} - P_B)^2$ is the momentum transfer. Their result is

$$F(q^2) = F(0) \left(1 - \frac{1}{6} \langle r^2 \rangle q^2 \right), \quad (56)$$

where $\langle r_v^2 \rangle^{1/2} = 0.79 F$ in (Fermis) and q^2 is expressed in Fermis. They assume $\langle r_A^2 \rangle = \langle r_v^2 \rangle$, and $F_v = F_a$ for lack of any experimental information.

One set of values for the unknown quantities, which were derived from least squares fits from available data (Frazer, 1966) is

$$\Theta = 0.254 \text{ radians, } f_A = 0.437, \quad d_A = 0.742.$$

In Table I are listed the matrix $j^{(H)}$ that are of interest here (from Frazer 1966, Table 8.3).

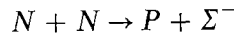
Now

$$\begin{aligned} H_{\text{int}} &= j_\lambda^{(H)} j^{\lambda(H)\dagger} + j_\lambda^{(L)} j^{\lambda(L)\dagger} + j_\lambda^{(H)} j^{\lambda(L)\dagger} + (\text{complex conjugate}) \\ &= j_\lambda^{(0)H} j^{\lambda(1)H\dagger} + \dots \end{aligned} \quad (57)$$

TABLE I
V-A matrix elements

	V	A
Pn	$\cos \theta$	$(f_A + d_A) \cos \theta$
A^0P	$-\sqrt{\frac{3}{2}} \sin \theta$	$-\sqrt{\frac{3}{2}}(f_A + \frac{1}{3}d_A) \sin \theta$
Σ^-n	$-\sin \theta$	$-(f_A - d_A) \sin \theta$
Σ^-A^0	0	$\sqrt{\frac{2}{3}} d_A \cos \theta$

For the reaction



we get from the coupling of the hadronic currents

$$H_{\text{int}} = -\frac{G}{\sqrt{2}} F(q^2) \sin \Theta \cos \Theta \bar{\psi}_p \gamma_\lambda (1 - r\gamma_5) \psi_N \bar{\psi}_\Sigma \gamma^\lambda (1 - s\gamma_5) \psi_N, \quad (58)$$

where

$$\begin{aligned} r &= f_A + d_A = 1.179, \\ s &= f_A - d_A = -.305. \end{aligned}$$

We can now write M in terms of the spinors in momentum space

$$\begin{aligned} M &= -\frac{G}{\sqrt{2}} F(q^2) \sin \Theta \cos \Theta [\bar{u}_p \gamma_\lambda (1 - r\gamma_5) u_N] \\ &\quad \times [\bar{u}_\Sigma \gamma^\lambda (1 - s\gamma_5) u_N]. \end{aligned} \quad (59)$$

We now evaluate $|M|^2$ by summing over final spins and averaging over the initial spins

$$\begin{aligned} |M|^2 &= \frac{G^2}{2} |F(q^2)|^2 \sin^2 \Theta \cos^2 \Theta \frac{1}{2} \\ &\quad \times \sum_{\substack{s_i \\ s_f}} \bar{u}_p \gamma_\lambda (1 - r\gamma_5) u_N \bar{u}_\Sigma \gamma^\lambda (1 - s\gamma_5) u_N \bar{u}_N \gamma^\mu (1 - s\gamma_5) \\ &\quad \times u_{\Sigma^-} \bar{u}_N \gamma_\mu (1 - r\gamma_5) u_p. \end{aligned} \quad (60)$$

The evaluation of $|M|^2$ is straightforward but tedious and is left to Appendix C. Using $r=1.179$, $s=-.305$, $m_4=1197$ and $m_1=m_2=m_3=940$, Equation C-10 becomes

$$|M|^2 = 2.34P_1 \cdot P_2 P_3 \cdot P_4 + 8.10P_1 \cdot P_4 P_2 \cdot P_3 - 9.81 \times 10^{11} + 2.46 \times 10^6 P_1 \cdot P_3 - 3.77 \times 10^5 P_2 \cdot P_4. \quad (61)$$

We can simplify the evaluation of $|M|^2$ by noting the following restrictions on Fermi momentum and energy in a degenerate gas.

Now $|\mathbf{P}_3| |\mathbf{P}_4|/E_3 E_4 \lesssim .04$, $|\mathbf{P}_1| |\mathbf{P}_4|/E_1 E_4 \lesssim .1$, and the angle between the neutrons is restricted to a small range $\sim 160^\circ$ to 170° (i.e. $|\mathbf{P}_y - \mathbf{P}_p| \leq |\mathbf{P}_n + \mathbf{P}_n| \lesssim |\mathbf{P}_y + \mathbf{P}_p|$).

Also using

$$\begin{aligned} E_1 &\doteq E_2, & |\mathbf{P}_1| &= |\mathbf{P}_2| \\ P_3 \cdot P_4 &= \mathbf{P}_3 \cdot \mathbf{P}_4 - E_3 E_4 \doteq -E_3 E_4 \\ P_1 \cdot P_4 &= P_2 \cdot P_4 \doteq -E_1 E_4 \\ P_1 \cdot P_3 &= P_2 \cdot P_3 \doteq -E_2 E_3 \end{aligned} \quad (62)$$

and

$$\begin{aligned} q^2 &= (P_4 - P_2)^2 \simeq -m_4^2 - m_2^2 + 2E_4 E_2 \\ P_1 \cdot P_2 &= \mathbf{P}_1 \cdot \mathbf{P}_2 - E_1 E_2 = -(.97|\mathbf{P}_1|^2 + E_1^2). \end{aligned}$$

we can simplify Equation (61)

$$|M|^2 \doteq 2.34(.97|\mathbf{P}_1|^2 + E_1^2) E_3 E_4 + 8.10E_1^2 E_3 E_4 - 9.81 \times 10^{11} - 2.44 \times 10^6 E_1 E_3 + 3.77 \times 10^5 E_1 E_4. \quad (63)$$

We can now write out an expression for the reaction rate

$$\begin{aligned} \frac{dn}{dt} &= \frac{G \sin^2 \Theta \cos^2 \Theta}{4(2\pi)^5} (kT)^4 |F(q^2)|^2 \frac{c}{(\hbar c)^4} I(\Delta) \\ &\times \{2.34(.97|\mathbf{P}_1|^2 + E_1^2) + 8.10E_1^2 E_3 E_4 - 9.81 \times 10^{11} \\ &- 2.44 \times 10^6 E_1 E_3 + 3.77 \times 10^5 E_1 E_4\} \text{cm}^{-3}\text{-sec}^{-1} \end{aligned} \quad (64)$$

where we introduce $c/(\hbar c)^4$ to put dn/dt in the proper units ($\hbar c = 1.97 \times 10^{-11}$ MeV-cm), and we evaluate E and P at the top of the Fermi sea. Now $G = 10^{-5}/M_p^2$ and $\sin \Theta = .26$, hence for the net reaction rate (forward-reverse) $dn/dt = 4.15 \times 10^{25} (kT)^4$

$$|F(q^2)|^2 (I(\Delta) - I(-\Delta)) \times \{\dots\} \text{cm}^{-3}\text{-sec}^{-1}. \quad (65)$$

Later we will see how to use the reaction rates with a vibrating neutron star.

D. Δ^- REACTION RATES

The model we use for the reaction $N+N \rightarrow P+\Delta^-$ is a modified one pion exchange, and is represented diagrammatically in Figure 5.

We can again start from the S matrix and perform the same phase space calculation as in the Σ^- reactions, it, therefore, remains only to solve for the transition matrix M .

In recent years, the one pion exchange peripheral model has received much atten-

tion in studying resonances. Work by Selleri (1961) and Jackson and Pilkuhn (1964) has led to analytic expressions for M and cross sections, for resonance scattering mediated by various meson types. A one pion exchange (OPE) gives too large a result at large momentum transfers, and form factors are introduced to correct for this (Jackson and Pilkuhn discuss other possible approaches besides form factors to correct the OPE model).

The Δ^- reaction we study is mediated by a pseudoscalar meson (π^-) and the transition matrix can be written (neglecting exchange terms)

$$M = G_1 \bar{u}(p_3) \gamma_5 u(p_1) \frac{F(t)}{m_{\pi^-}^2 - t} \frac{G_2}{m_{\pi^-}} \bar{u}(p_4) p_{2\gamma} u(p_2), \quad (66)$$

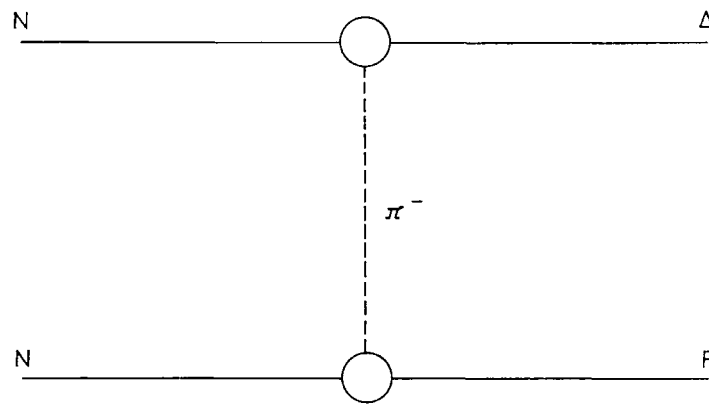


Fig. 5. One pion exchange diagram for the Δ^- reaction.

where G_1 and G_2 are the coupling constants at their respective vertices (they are not necessarily equal), $F(t)$ is the form factor, $(m^2 - t)^{-1}$ is the pion propagator, and t is the momentum transfer. Letting \sum refer to a sum over the final spins and over the initial spins, we can write

$$|M|^2 = \frac{G_1^2 G_2^2}{m_{\pi^-}^2} \frac{|F(t)|^2}{(m_{\pi^-}^2 - t)^2} \sum |\bar{u}(p_3) \gamma_5 u(p_1)|^2 \sum |\bar{u}(p_4) p_{2\gamma} u(p_2)|^2. \quad (67)$$

The form factor can be written as

$$F(t) = \frac{\alpha^2 - m_{\pi^-}^2}{\alpha^2 - t}, \quad (68)$$

where $\alpha^2 = 0.13 \times 10^6$ (MeV/c)² is found from a fit to experimental data (Jackson and Pilkuhn, 1964), $u(P_4)$ is the spinor representation for a spin $\frac{3}{2}$ particle.

Now

$$\frac{dn}{dt} = \frac{1}{6(2\pi)^5} (kT)^4 I(\Delta) \frac{G_1^2 G_2^2}{m_{\pi^-}^2} \frac{c}{(\hbar c)^4} \times \left[\frac{\alpha^2 - m_{\pi^-}^2}{\alpha^2 - t} \right]^2 \frac{(m_2^2 - E_2^2)}{(m_{\pi^-}^2 - t)^2} (t - (m_1 + m_2)^2) (t - (m_1 - m_3)^2). \quad (69)$$

For π^- emission at a nucleon-nucleon vertex $G^2/4\pi \simeq 30$. We can estimate the coupling constant at the resonance vertex by use of the decay width relation (Jackson and Pilkuhn, 1966, page 911; Colleraine 1967, page 33)

$$\Gamma_{c \rightarrow ac} = \frac{2}{3} \frac{G_2^2}{4\pi} \frac{p^3}{m_c^2}, \quad (70)$$

where the decay is in the rest frame. Using (Rosenfeld, 1967) $\Gamma = 120$ MeV for $\Delta^- \rightarrow N + \pi^-$ we find $G_2^2/4\pi \simeq 22$. Since $m_1 \simeq m_3$ we have

$$\begin{aligned} \frac{dn}{dt} = & 2.42 \times 10^{49} (kT)^4 \left[\frac{\alpha^2 - m_\pi^2}{\alpha^2 - t} \right]^2 t \\ & \times \frac{(t - 4m_1^2)(m_1^2 - E_1^2)}{(m_\pi^2 - t)^2} \{I(\Delta) - I(-\Delta)\}. \end{aligned} \quad (71)$$

E. Λ^0 REACTIONS

There are several reactions which can produce the Λ^0 particle in a neutron star. These are



The first is a weak interaction, and the latter are strong interactions. For (72) we can solve for the rate using the expression for the Σ^- except $r = 1.179$, $s = 0.684$ and $m_{\Lambda^0} = 1.115 \times 10^3$ MeV. The strong interactions can be estimated by our modified one pion exchange model. These reactions all occur at the same threshold in the star. Since the Λ^0 can be produced in a strong interaction it will proceed rapidly. As will be discussed later such rapid reactions do not contribute to damping and we will not pursue any exact calculations of the rates.

3. Vibrating Neutron Stars

Static solutions of neutron stars have been constructed by Tsuruta and Cameron using a realistic equation of state. They include in the equation of state the effects of nuclear forces by using the V_β and V_γ Levinger and Simmons (1961) nuclear potentials. In an independent particle model Σ^- particles will be present in large numbers at a density threshold of 10^{15} g/cm³. Some of the models constructed had densities high enough to contain hyperons in the central region of the star. It is for these stars that we can find damping due to hyperon reactions.

Hansen and Tsuruta studied six representative neutron star models including vibrations and damping by URCA mechanisms. The density profiles of these stars are shown in Figures 6 and 7, and their properties are summarized in Table II. M_\odot

is the solar mass, M the neutron star mass, ρ^c is the central density, τ is the period and a_v is a coefficient in the vibrational energy expression $E_v = a_v \varepsilon^2$. ε is the fractional perturbation at maximum amplitude of the radius in the $n=0$ mode (i.e. $\delta r = \varepsilon r e^{i\omega t}$).

4. Damping

A. INTRODUCTION

In the previous sections, we have evaluated non-equilibrium reaction rates for sample weak hyperon and strong resonance reactions in a neutron star, and we mentioned

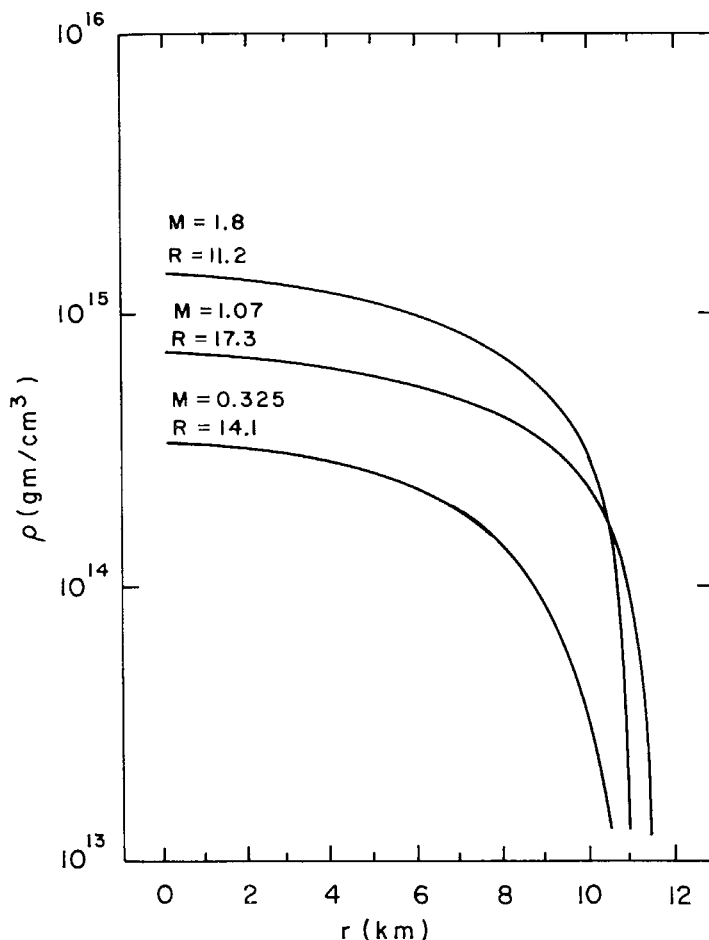


Fig. 6. Density profiles for three V_β neutron stars. M is mass in M_\odot and R is the radius in km.

the vibrational structural aspects of neutron stars. We now bring these topics together to show how rapidly these reactions can damp the vibrations; we answer the question, if we start a neutron star vibrating can it continue to vibrate for astronomical times?

When calculating neutrino damping one can consider the neutrinos to be escaping from the star, or at least some fraction escaping, with the rest feeding back into the star. This latter complication is not as severe as the one we face here. The reactions

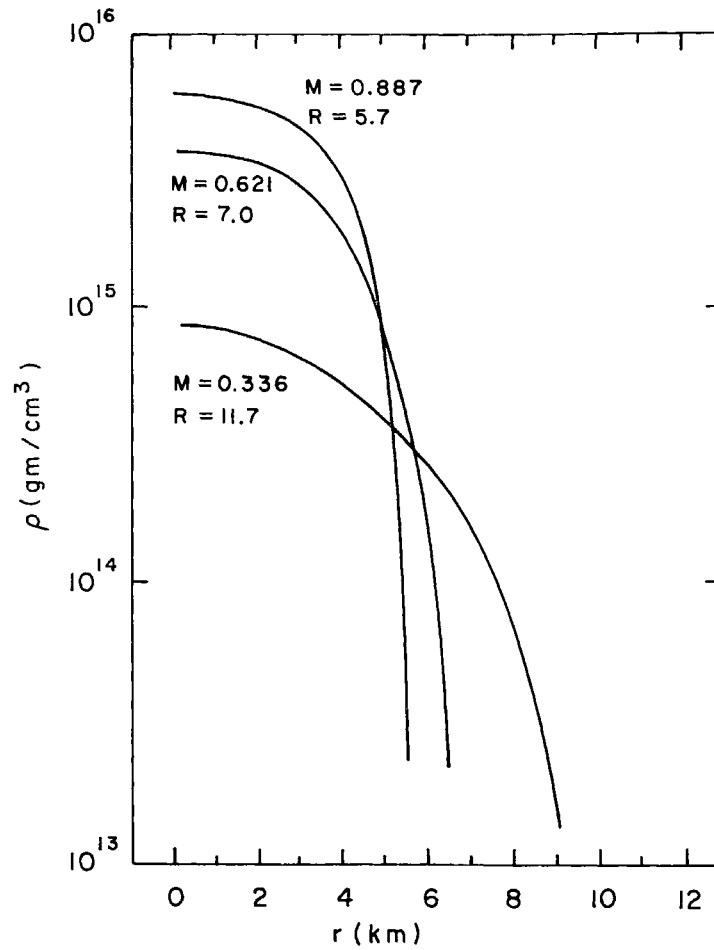


Fig. 7. Same as Figure 6 except that a V_γ potential was used.

TABLE II
Neutron star properties

Potential	M/M_\odot	$R(\text{km})$	$\rho^c (\text{gm}/\text{cm}^3)$	$\tau (10^{-3} \text{ sec})$	$\text{Log } a_v (\text{ergs})$
V_γ	1.801	11.22	1.364×10^{15}	0.50	53.7689
V_γ	1.074	12.33	6.89×10^{14}	0.375	53.5305
V_γ	.3249	14.15	3.258×10^{14}	0.50	52.4640
V_β	.8874	5.733	6.194×10^{15}	0.50	52.8518
V_β	.5927	7.159	3.55×10^{15}	0.265	53.0055
V_β	.3361	11.66	8.717×10^{14}	0.625	52.1145

of interest to us do not radiate energy; rather they dissipate the vibrational energy through thermal heating. Let us discuss this process in more detail.

Imagine a box containing a gas composed of one type of particle in which we vary one dimension sinusoidally. This variation corresponds to increasing and decreasing the volume by pulling out and pushing in one wall. If the temperature is held constant, the work done in a cycle is zero. Through part of the cycle we do work on the box,

and through the remainder of the cycle the box does the same amount of work on us. Here the pressure is a simple function of the volume.

To study the work done in a cycle, we look at a pressure-volume (PV) diagram, with

$$W = \oint P \, dV, \quad (75)$$

where W is the work and P the pressure.

The area under a PV diagram tells how much work is done, and the direction of the cycle tells us whether work is done on the system or if the system itself does work.

When we consider a gas composed of several particle types, with reactions between them, we find that work can be performed in a cycle. Now as we displace the volume of the box, the equilibrium configuration is different from the initial one. The reactions between the particles now proceed in a direction to satisfy the new equilibrium state. However, we are continuously varying the volume (equilibrium state) and the system is always trying to adjust from its present state to the equilibrium state. Now the pressure as the volume increases will not go through the same path as when the volume decreased.

If there were no reactions between particles, we would expect the PV diagram shown in Figure 8(a). With reactions, however, a dissipative PV cycle will look like Figure 8(b).

The amount of work done on the system during a cycle is a sensitive function of the reaction rates and the frequency of oscillation of the system. If the reaction rates are very slow compared to the driving frequency, then the system will change very little between compression and expansion, hence very little work will be done. When comparing reaction rates to the driving frequency, we are actually concerned with the frequency with which a particle undergoes a reaction. When the reaction rates are very fast, the gas adjusts rapidly to equilibrium and the PV curve traces back close to itself through the cycle and very little work is done. Obviously, the two extreme cases of zero and infinite reaction rates represent ideal cases of no work.

In the intermediate case, where the particles can interact on the order of 10^{-2} to 10^2 times per cycle, damping is rapid. To see what happens we follow a PV cycle from equilibrium at $\omega t = 0$. During compression the equilibrium state is that of a higher density gas composed of more hyperons. The reactions proceed in the direction of this higher pressure state (higher than the no reaction gas case). At full compression ($\omega t = \pi/2$) the reaction rates have not been sufficient to restore equilibrium. As the mechanical system returns to $\omega t = \pi$ the thermodynamic equilibrium goes toward a lower pressure. The actual system, however, is not yet at equilibrium and the reactions keep increasing the actual pressure. At some point equilibrium is satisfied, but when the system has returned to $\omega t = \pi$ there is an excess of pressure over the equilibrium state ($\omega t = 0$). The process from $\omega t = \pi$ to $\omega t = 2\pi$ (expansion) is similar except that the pressure is lower. The result is a PV diagram like that in Figure 8(b). For large damping there is a significant lag between the equilibrium state and the actual state over much of the cycle.

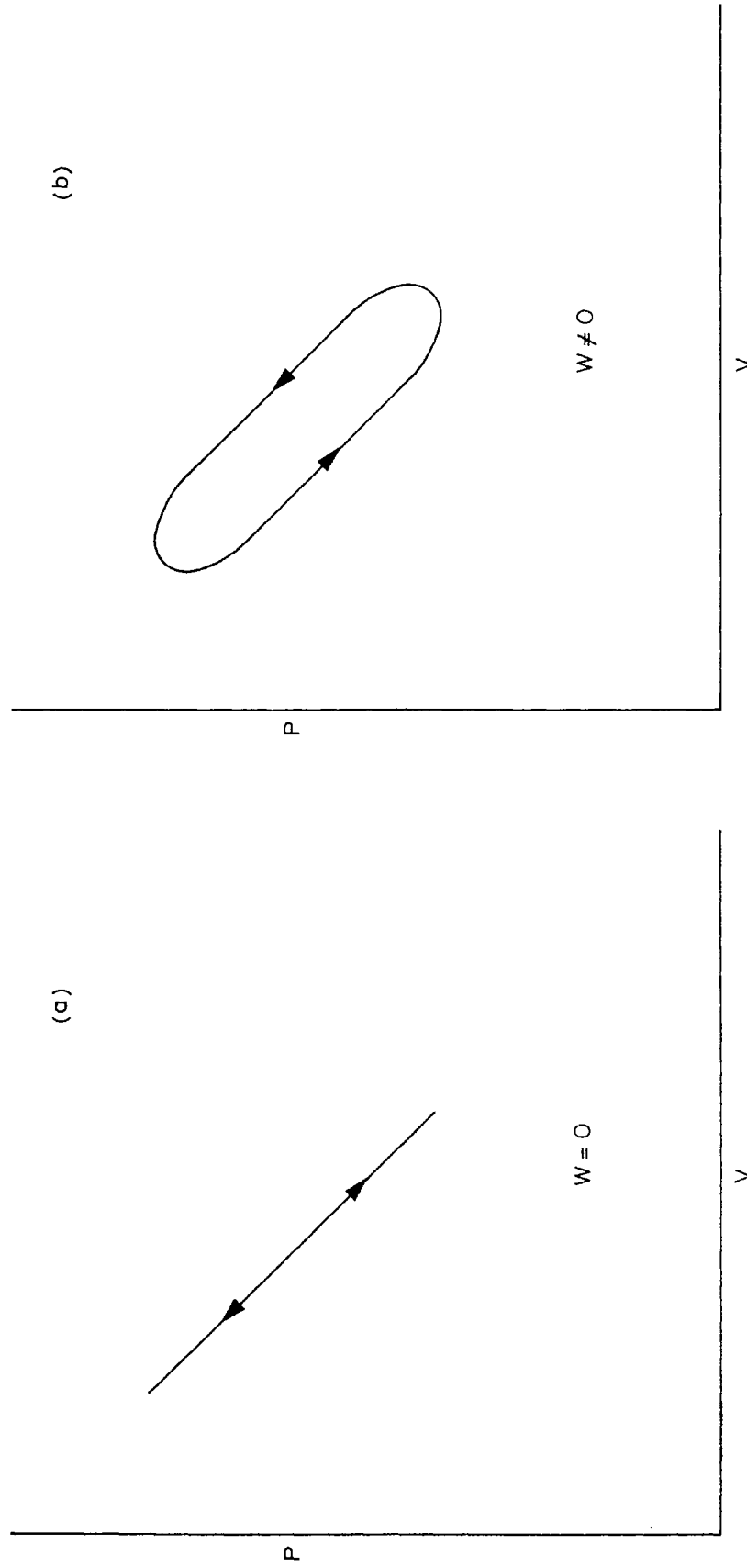


Fig. 8. (a) PV diagram for no reaction case, W (Work)=0. -- (b) PV diagram for reactions with damping.

We find the Δ^- reaction rates to be very rapid (twenty orders of magnitude faster than the Σ^- rates) and these reaction play no significant role in producing work. Only reactions which involve a weak interaction can be important in thermal damping; more will be said of this later.

An analog to the system we have here is a driven harmonic oscillator with damping. We can imagine ourselves mechanically varying the volume of the box, with the reactions, in the box damping out the vibrations through heating.

The equation for a driven damped harmonic oscillator is

$$\ddot{x} + \gamma\dot{x} + \omega^2x = \frac{F_0}{m} \cos(\omega t + \theta_0). \quad (76)$$

The average power (the rate at which work is done) over a cycle for Equation (76) is

$$P_{av} = \frac{F_0^2 \omega \cos \beta}{2m [(\omega^2 - \omega_0^2)^2 + 4\gamma^2 \omega^2]^{1/2}}, \quad (77)$$

where β is a phase

$$\beta = \tan^{-1} \frac{\omega_0^2 - \omega^2}{2\gamma\omega}. \quad (78)$$

Typical results are shown in diagram (9).

B. DAMPING

Finding the work done, when nonequilibrium reaction rates are present, is a nonlinear problem. In order to calculate the work done during a cycle, we must know the pressure, P , as a function of time, but

$$P = P(N_i(t)) \quad (79)$$

and we only need to know the number density as a function of time. But symbolically

$$N = N\left(t, \frac{dn}{dt}\right) \quad (80)$$

and from Equation (65) we know that

$$\frac{dn}{dt} = F(E_i(t)). \quad (81)$$

However,

$$E_i = E_i(N_i(t)) \quad (82)$$

and their relationships are nonlinear.

The solution to this problem was generated on a computer for a range of amplitudes and frequencies. Simultaneously with the solution for $N(t)$, we calculated $P(t)$ and the work done in a cycle.

The variations about the equilibrium radius are described by

$$\xi(r, t) = \xi_0(r) e^{i\omega t}, \quad (83)$$

where $\xi_0(r) \simeq \delta r / r_0 \simeq \text{constant}$; hence,

$$r = (1 + \xi_0 e^{i\omega t}) r_0 \quad (84)$$

and the density is

$$\varrho(t) = \varrho_0 (1 + \xi_0 \sin \omega t)^{-3}. \quad (85)$$

Similarly, the local number densities for the different particle species are

$$N_i(t) = N_i(0) (1 + \xi_0 \sin \omega t)^{-3}. \quad (86)$$

When we include the reactions, where dn/dt is in units of $\text{cm}^{-3} \text{sec}^{-1}$, we have

$$N_i(t) = \left\{ N_i(0) + \int_0^t \frac{dn_i}{dt} dt \right\} (1 + \xi_0 \sin \omega t)^{-3}. \quad (87)$$

Once we know $N_i(t)$ we can calculate the Fermi momenta and energy, and then the pressure as a function of time. We also know how the volume varies with time and can calculate $dV(t)$

$$dV(t) \simeq dV(0) 3\omega \xi_0 \cos \omega t. \quad (88)$$

We can improve the accuracy of our solution if we expand about the equilibrium value and consider only the variations. Subtracting off the constant part of the pressure does not change the calculation of the work

$$W = \oint \Delta P(t) dV, \quad (89)$$

but improves the accuracy when integrating around the PV diagram with a computer. Expanding we have

$$\begin{aligned} N_i(t) &= (1 + \xi_0 \sin \omega t)^{-3} \int_0^t \frac{dn_i}{dt} dt \\ &+ N_i(0) \sum_0^{\infty} \frac{(-1)^j (j+2)!}{j! 2!} (\xi_0 \sin \omega t)^j. \end{aligned} \quad (90)$$

Therefore,

$$\begin{aligned} \Delta N_i(t) &= (1 + \xi_0 \sin \omega t)^{-3} \int_0^t \frac{dn_i}{dt} dt \\ &+ N_i(0) \sum_1^{\infty} \frac{(-1)^j (j+2)!}{j! 2!} (\xi_0 \sin \omega t)^j \end{aligned} \quad (91)$$

where $\Delta N = N_i(t) - N_i(0)$. We can use the series for $\zeta \lesssim 5 \times 10^{-2}$ as it holds for $\zeta < 1$. We must be careful to include enough terms in the series to correspond to the computer's accuracy.

For the Fermi momentum, p_i

$$p_i(t) = m_e \left(\frac{6N_i(t)}{a_0(2I_i + 1)} \right)^{1/3}, \quad (92)$$

where m_e is the electron mass, I_i the spin and N_i the number density of particle i and $a_0 = 1.76 \times 10^{30} \text{ cm}^{-3}$. We can now do a similar expansion for p , the Fermi energy E_F and finally the pressure P .

$$P = \sum_i P(i), \quad (93)$$

where $P(i)$, the partial pressure of particle i is,

$$P(i) = (2I + 1) \left(\frac{m}{m_e} \right)^4 \frac{a_1}{48} f(x) \left\{ 1 + \frac{4\pi^2}{\beta^2} \frac{xu_F}{f(x)} + \frac{7\pi^4}{15\beta^4} \frac{u_F(2x^2 - 1)}{f(x)x^3} \right\}, \quad (94)$$

$$x = p/m,$$

$$u_F = (1 + x^2)^{1/2},$$

$$g(x) = u_F x (2x^2 + 1) - \ln(x + u_F), \quad (95)$$

$$f(x) = 8x^3 u_F - 3g(x),$$

$a_1 = 1.44 \times 10^{24} \text{ ergs/cm}^3$ (or dyn/cm^2) and x and u are the dimensionless Fermi momentum and energy.

With Equation (91) and the reaction rate Equation (65) for the Σ^- reaction (4), we solve for $N_i(t)$ on a computer. Starting in equilibrium at $t=0$, we can then iterate in time, choosing iterations small enough so that $\Delta N(t_n)$ changes less than some fraction of $N(t_{n-1})$ (typically the fraction is $\lesssim 10^{-3}$), simultaneously evaluating Equation (89).

C. RESULTS FOR Σ^- DAMPING

The calculations were done for a sample volume in the core where Σ^- particles are present, as only the Σ^- reaction was considered (this choice is explained in the next section).

Since we are subtracting large values of the pressure which differ by small amounts, we ran a check on the program. Simultaneously with the reaction case, we calculated the work done by the no reaction case ($dn_i/dt=0$); here we expect zero work. The program was run in double precision on an IBM 7094. Because of roundoff errors, the computer gave a non-zero answer for the work done in the no reaction case; however, this value was ten to twelve orders of magnitude smaller than the work done in the reaction case. We feel that the program works well, giving effectively zero work during a cycle of the no reaction case.

There are several results and behavior patterns to look for if our explanation of

the damping is an accurate one. The most important result is the behavior of the system when the amplitude of vibration is fixed and the frequency is varied. If the program is working and the problem has been correctly set up and described, then the rate at which work is done per cycle should resemble the curves in Figure (9). The answers are physical; that is, as outlined before, if reactions are slow compared to ω , the work done is small; similarly, if reactions are fast, the system stays in equilibrium and little work is done. At fixed amplitude and for varying ω we expect a resonance behavior with damping. In the intermediate case, when the reaction frequency is comparable to the driving frequency, damping should be large.

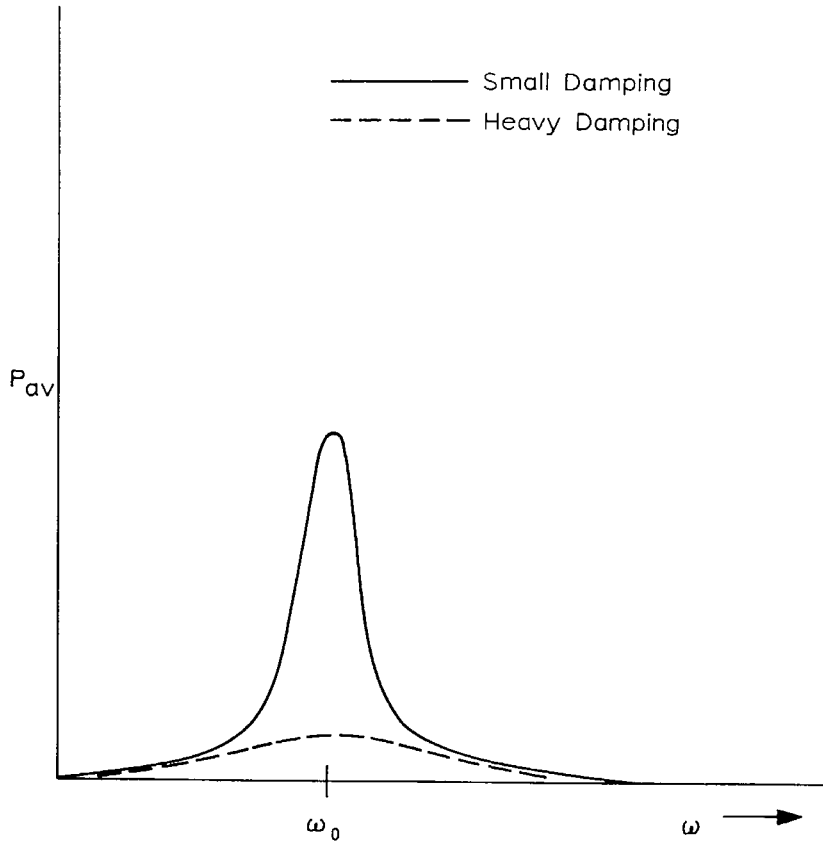


Fig. 9. Average power absorbed per cycle versus ω for a damped driven harmonic oscillator.

The results of fixing ξ and varying ω are shown in Figures 10, 11, 12 for three different values of ξ . We see that we do get a resonance effect as we vary ω . We also see that when we go to larger amplitudes the damping increases, and, as would be expected, the curves broaden. At small amplitudes, the natural frequency of the neutron star is far from the damping resonance frequency, and the system will damp slowly. As we go to larger amplitudes, the damping resonance frequency increases, eventually coinciding with the natural frequency of vibrations at $\xi \simeq 2.5 \times 10^{-2}$, and finally shifting above it at larger amplitudes.

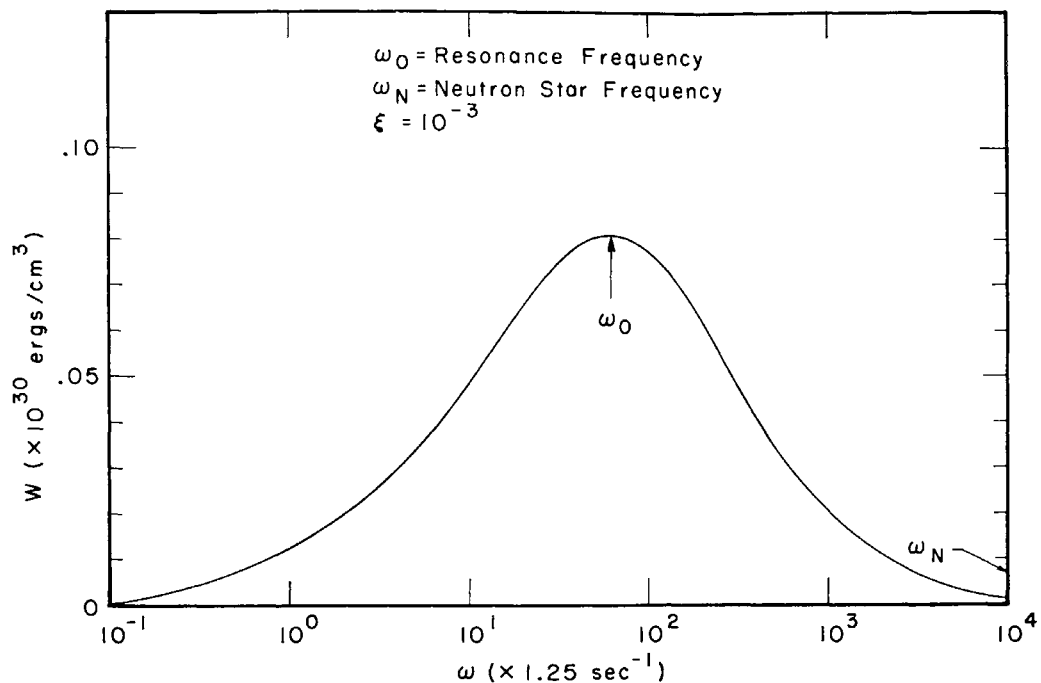


Fig. 10. Work per cycle for a sample volume in a vibrating neutron star versus ω , for a fixed perturbation ξ . The damping is by the $N+N \rightleftharpoons P + \Sigma^-$ mechanism.

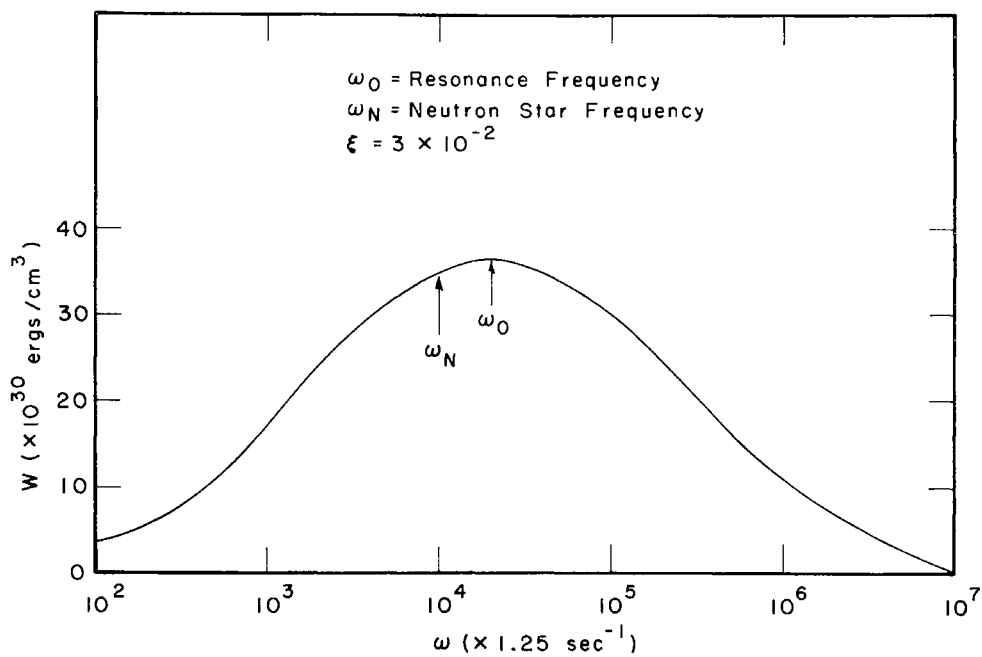


Fig. 11. Same as Figure 10.

These results establish the nature of the damping and confirm the ability of the program to reproduce physical results over a wide range of frequencies and amplitudes.

Next we fixed the frequency at that of the natural frequency of a neutron star (a sample star with a hyperon core was chosen, the V_γ , $M=1.8 M_\odot$ model, see Table II herein, described by Hansen and Tsuruta, and the amplitude was varied to find $\Delta\varepsilon/\varepsilon$ versus ξ .

Initially the system is at equilibrium, as the volume increases the pressure decreases; after $\omega t = \pi/2$ the volume decreases and the pressure increases, but P is at a higher value than the first quarter of the cycle. This system absorbs energy (i.e., damps the

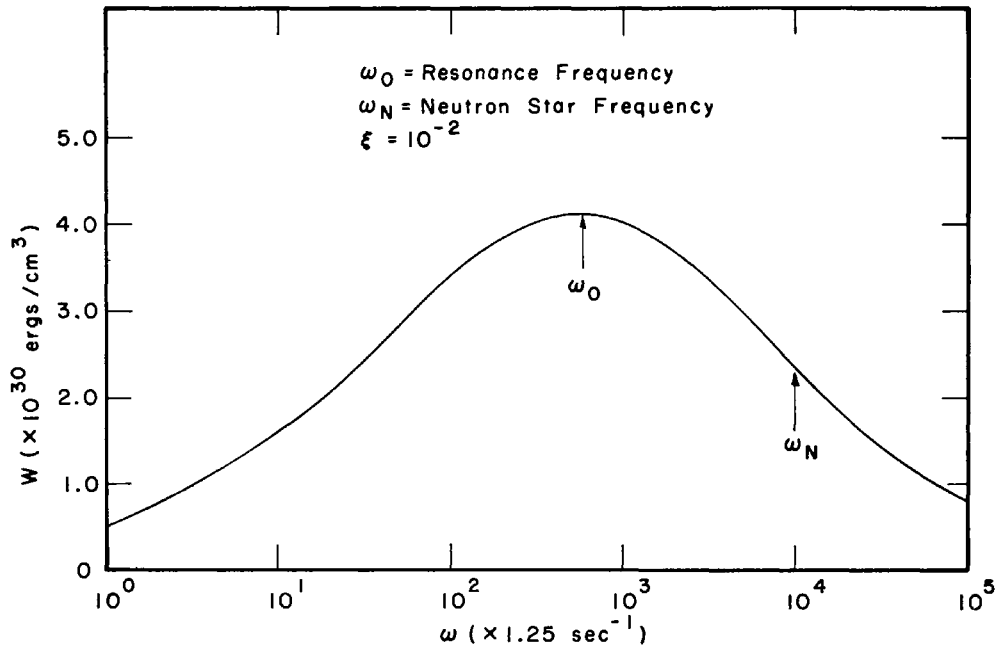


Fig. 12. Same as Figure 10.

mechanical energy) and converts it to thermal heat. Had the cycle gone in the other direction in time, heat would have been converted into mechanical energy and an instability would be achieved. As a check, the cycle was run 180° out of phase (at $t=0$ we decrease the pressure) to see if the system gave a work cycle, where mechanical energy is converted to thermal energy. We found this to be the case, and the answers were the same as the original situation. Our program, corresponding to what we expect physically, is insensitive to which way the system is driven.

Finally we applied these results to our sample star and followed its energy as a function of time from some initial amplitude. As the energy stored decreases, ξ decreases and the damping rate decreases, eventually going asymptotically to zero. The results are shown in Figure 13 (one second equals 2×10^3 cycles). The calculations include damping only in the hyperon core (region where hyperons are present), and

ε is the total energy of the star as a function of time. The hyperon core radius is 5×10^3 m compared to the star radius of 1.1×10^4 m.

The calculations performed show that the Σ^- reaction (4) damps out the vibrational energy of the neutron star in a short time. Only very small amplitudes, much less than $\xi = 10^{-8}$, can survive for astronomical times. However, at $\xi < 10^{-8}$, a typical V_γ star would store less than $\sim 6 \times 10^{37}$ ergs, and the estimated rate (for example) of electromagnetic radiation from the Crab nebula is $\sim 10^{38}$ erg sec $^{-1}$.

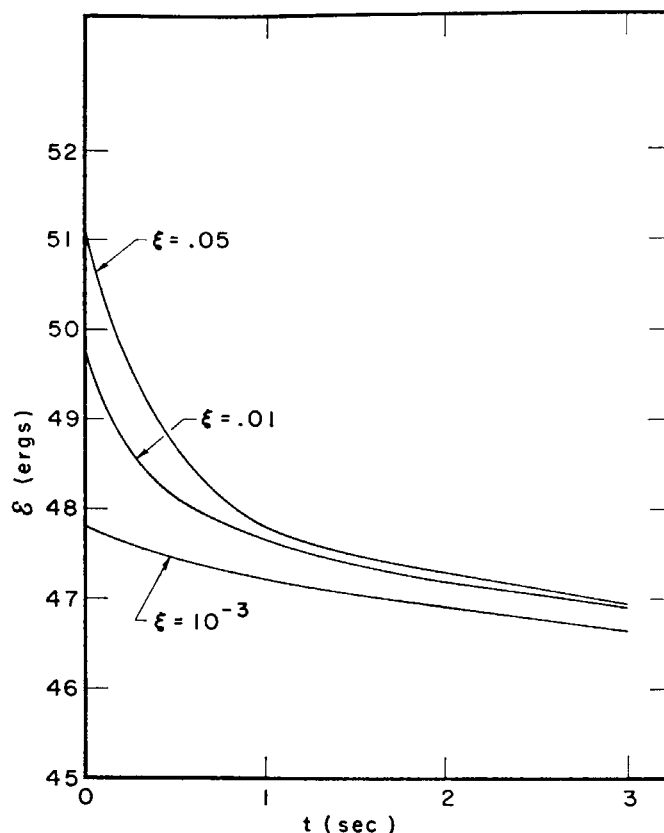


Fig. 13. Vibrational energy of the $M=1.8 M_\odot V_\gamma$ neutron star versus time when damping is present (1 sec equals 2×10^8 cycles).

There is a final point about the role of temperature which should be mentioned. Bahcall and Wolf (1965b) found that a neutron star's atmosphere will cool to between 10^6 and 10^7 K in less than 10^{-2} years after formation. From the work of Tsuruta (1964), the core temperature is two orders of magnitude higher. For all the calculations here, we chose the temperature at 10^9 K ($kT = .086$ MeV), which should be typical of a neutron star interior.

During a cycle, we assumed that T remains constant; in fact this is not so, but the change is so small as not to be a significant factor. We calculate the work done in a cycle and then calculate the change in temperature due to the increase in the thermal energy.

For the V_γ , $M=1.8 M_\odot$ neutron star,

$$E_{th} = 1.55 \times 10^{30} T^2 \quad (96)$$

where E_{th} is the thermal energy in ergs and T is the temperature in K (Hansen and Tsuruta, 1967). The variations of the pressure occur mostly in the $T=0$ part of the expansion for the pressure. The significant role of the temperature is in the amount of phase space available for the nonequilibrium reactions.

Since it is possible to store up to five orders of magnitude more energy in vibrational motion than in thermal heat, the temperature will change significantly after several seconds of damping. When $\xi = 10^{-2}$ and $T(0) = 10^9$ K, the temperature after damping will be $\sim 6 \times 10^9$ K.

5. Epilogue

A. COMPARISON TO URCA RATES

According to the independent particle model, the Σ^- is the first hyperon to appear as the density increases in a neutron star. Reaction (4) is the most important damping mechanism in stars with cores dense enough to contain hyperons. If the central density is below the Σ^- threshold, the star damps by neutrino mechanisms (the URCA process). We shall see that the other hyperons (in the independent particle model) are not important for damping because of strong interactions.

In Hansen and Tsuruta (1967) five of the six models studies with neutrino damping still had enough energy after 10^3 years to supply X-ray sources with energy to account for their outputs. Σ^- damping eliminates three of the five models, which have hyperon cores (V_γ , $M=1.8 M_\odot$; V_β , $M=.89 M_\odot$; and V_γ , $M=.59 M_\odot$).

For comparison, we have calculated the neutrino URCA rate from Hansen (1966) and the Σ^- rate above threshold, when $\Delta \simeq 20$ (at $kT = .086$ MeV, $\Delta E = 1.72$ MeV). $(dn/dt)|_{URCA} \simeq 10^{30}/\text{cm}^3\text{-sec.}$ and $(dn/dt)|_{\Sigma^-} \simeq 2 \times 10^{39}/\text{cm}^3\text{-sec.}$

Hansen's original calculation using a one pion exchange (OPE) model, for the strong interaction part of the matrix, was six times larger than the results of Bahcall and Wolf (1965b). Bahcall and Wolf wrote the matrix elements in terms of the overlap between the initial and final state nucleon wave functions. The disagreement is due to Hansen neglecting form factors at the vertices. Using the expression for $F(t)$ in Equation (41), we find, at the momentum transfers involved in Hansen's reactions, that $|F(t)|^2 \simeq \frac{1}{6}$. Since to some degree, OPE and nuclear potential solutions to scattering have degrees of freedom which are fitted to the data, it is not surprising that the two methods yield similar results.

Why are the hyperon and URCA rates so different, when basically they are both weak interactions? To answer this, we recall our discussion of phase space. It is the fermions near the top of the degenerate sea which participate in inelastic scattering. Only a small fraction of the fermions interact; an order of magnitude estimate of the percentage of particles available is $kT/(E_F - mc^2)$. As $kT \ll (E_F - mc^2)$, the fewer the particles involved in a reaction process the faster it will go; the URCA reaction has six particles, the Σ^- only four. Secondly, the URCA process involves two interactions

(strong and weak) and the rates are a product of two reaction probabilities. The Σ^- reaction involves only a weak interaction.

B. STRONG INTERACTION REACTIONS

We have already stressed why the slow weak interaction Σ^- rates for



are important in damping, and why the fast strong interaction Δ^- rates are not. It is important to know whether there exist any strong interaction reactions for producing hyperons. Wherever these strong reactions are available, the hyperons would interact rapidly and would no longer contribute to damping.

The Σ^- particles are present in the core above $\rho \doteq 1.05 \times 10^{15} \text{ g/cm}^3$, the next particles to appear, at $\rho \doteq 1.90 \times 10^{15} \text{ g/cm}^3$, are the Λ^- and Λ^0 .

Some possible strong (strangeness conserving) interactions involving these particles are,



The threshold for reaction (65) is $\rho \doteq 1.90 \times 10^{15} \text{ g/cm}^3$ (the Λ^0 threshold), and for (66) at $\rho = 2.2 \times 10^{15} \text{ g/cm}^3$.

Between the Σ^- threshold and that of the Λ^0 and Δ^- , there is a slow hyperon reaction $N + N \rightleftharpoons P + \Sigma^-$ which rapidly damps vibrations. Once the Λ^0 threshold is reached, there are strong interaction hyperon reactions which proceed rapidly. These reactions are dominant and the system remains in equilibrium during vibrations, thus eliminating damping.

For the V_γ ($M = 1.8 M_\odot$) star, used as an example in the previous section, the Λ^0 threshold is never reached. Thus damping occurs throughout the hyperon core up to $r = 5 \text{ km}$; the central density, ρ_c , of this star, is $1.32 \times 10^{15} \text{ g/cm}^3$ and the Λ^0 threshold is at $\rho = 1.90 \times 10^{15} \text{ g/cm}^3$.

For the two V_β stars with hyperon cores the Λ^0 threshold is reached, and the density has a steeper rise in the Σ^- damping region than does the V_γ star. For V_β ($M = 0.89 M_\odot$) the damping layer, r , extends from 4.0 to 4.9 km, where the radius, $R = 7.0 \text{ km}$; for V_β ($M = 0.62 M_\odot$) r is from 4.4 to 4.8 km, with $R = 5.7 \text{ km}$. Typically, only 15% of the volume of the star contributes to the damping.

C. THRESHOLDS

From the previous discussion it is obvious that the thresholds for the appearance of the hyperons play a role in determining which stars have their vibrations rapidly damped. The calculation of the thresholds was based on an independent particle model, yet, we know that an interaction energy exists between baryons due to strong interactions.

From Wolf (1966), however, it seem likely that the threshold will be lower and the

hyperons will appear at a lower density (possible as low as $\rho \sim 6 \times 10^{14} \text{ g/cm}^3$). If the threshold is lower, hyperons will be present in more of the neutron star models.

If the Λ^0 and/or Δ^- has a lower threshold than the Σ^- our conclusions will not change. If the Λ^0 comes before the Σ^- particle then the damping reaction will be $N + P \rightleftharpoons \Lambda^0 + P$. The calculation of the reaction rate will be similar to that of the Σ^- . When the Σ^- threshold is reached, the fast reactions (due to strong interactions) dominate and there will be no damping beyond this density.

Basically, any vibrating neutron star with a hyperon core will damp rapidly, no matter which hyperon first appears. The first hyperon type must be created by a strangeness violating reaction and the rates for these reactions are of the right magnitude to cause rapid thermal damping.

The Δ^- has strangeness zero, and being created by a strong interaction, is not important for damping. We calculated the Δ^- rates to have an estimate of the rates for strong interactions in a neutron star, as well as to determine if the resonance particles could contribute to damping. No matter what its threshold the Δ^- is not important for damping.

E. CONCLUSION

In conclusion, any vibrating neutron star, with a hyperon core, rapidly damps down. The mechanism for damping is thermal heating due to a weak interaction hyperon reaction. In the independent particle model this hyperon is the Σ^- and the reaction is $N + N \rightleftharpoons \Sigma^- + P$. This work, as far as we know, is the first attempt to consider such damping, and uses the VA theory and Cabibbo's work.

Obviously, if neutron stars should be observed, then the results here may help limit the possible models.

For the future, when more is understood about hyperon-nucleon potentials, as well as nucleon-nucleon potentials, accurate neutron star models will be possible. The interactions may significantly change the thresholds for hyperon production, altering our view of dense matter, and possibly eliminating more vibrating models.

Appendix A: Evaluating $I(\Delta)$

$$I(\Delta) = \int_{-\infty}^{\infty} dx_3 \int_{-\infty}^{\infty} dx_2 \int_{-(x_2+x_3+\Delta)}^{\infty} dx_1 \prod_{i=1}^3 (1 + e^{x_i})^{-1} \\ \times \left[1 + e^{-\left(\sum_1^3 x_i + \Delta\right)} \right]^{-1} \left[\left(\sum_1^3 x_i + \delta \right)^2 - \beta^2 m_4^2 \right]^{1/2}. \quad (\text{A-1})$$

We employ the following transformations, whose Jacobian is one:

$$\left. \begin{aligned} y_1 &= x_1 + x_2 + x_3 & x_1 &= y_1 - y_2 \\ y_2 &= \quad x_2 + x_3 & \text{or } x_2 &= y_2 - y_3 \\ y_3 &= \quad \quad x_3 & x_3 &= \quad y_3 \end{aligned} \right\}, \quad (\text{A-2})$$

hence,

$$I(\Delta) = \int_{-\infty}^{\infty} dy_3 \int_{-\infty}^{\infty} dy_2 \int_{-\Delta}^{\infty} dy_1 [(y_1 + \delta)^2 - \beta^2 m_4^2]^{1/2} (1 + e^{y_3})^{-1} \\ \times (1 + e^{y_1 - y_2})^{-1} (1 + e^{y_2 - y_3})^{-1} (1 + e^{-(y_1 + \Delta)})^{-1}, \quad (\text{A-3})$$

where the lower limit on y_1 comes from

$$y_1|_{\min} = -(x_2 + x_3 + \Delta) + x_2 + x_3 = -\Delta.$$

First we perform the y_3 integral

$$\int_{-\infty}^{\infty} (1 + e^{y_3})^{-1} (1 + e^{y_2 - y_3})^{-1} dy_3 \\ = (1 - e^{y_2})^{-1} \int_{-\infty}^{\infty} dy_3 [(1 + e^{y_3})^{-1} - (1 + e^{y_3 - y_2})^{-1}]. \quad (\text{A-4})$$

In this form divergences appear in each term, but cancel when combined; the solution is best achieved by the following expansions:

$$y_3 < 0: (1 + e^{y_3})^{-1} = 1 + \sum_1^{\infty} (-1)^n e^{ny_3}, \\ y_3 > 0: (1 + e^{y_3})^{-1} = - \sum_1^{\infty} (-1)^n e^{-ny_3}, \\ y_3 < y_2: (1 + e^{y_3 - y_2})^{-1} = 1 + \sum_1^{\infty} (-1)^n e^{ny_3} e^{-ny_2}, \\ y_3 > y_2: (1 + e^{y_3 - y_2})^{-1} = - \sum_1^{\infty} (-1)^n e^{-ny_3} e^{ny_2}. \quad (\text{A-5})$$

The right-hand side of Equation (A-4) becomes equal to

$$(1 - e^{y_2})^{-1} \left\{ (y + \sum_1^{\infty} (-1)^n e^{ny_3}) \Big|_{-\infty}^0 \right. \\ \left. - \sum_1^{\infty} (-1)^n e^{-ny_3} \Big|_0^{\infty} - (y + \sum_1^{\infty} (-1)^n e^{ny_3} e^{-ny_2}) \Big|_{-\infty}^{y_2} \right. \\ \left. + \sum_1^{\infty} (-1)^n e^{-ny_3} e^{ny_2} \Big|_{y_2}^{\infty} \right\} \quad (\text{A-6})$$

$$= (1 - e^{y_2})^{-1} \left\{ \sum_1^{\infty} (-1)^n - y \Big|_{-\infty} + \sum (-1)^n - \sum (-1)^n \right. \\ \left. + y \Big|_{-\infty} - y_2 - \sum (-1)^n \right\} = \frac{-y_2}{(1 - e^{y_2})}. \quad (\text{A-7})$$

Now,

$$I(\Delta) = \int_{-\Delta}^{\infty} dy_1 [(y_1 + \delta)^2 - \beta^2 m_4^2]^{1/2} (1 + e^{-(y_1 + \Delta)})^{-1} \\ \times \int_{-\infty}^{\infty} y_2 (1 - e^{y_2})^{-1} (1 + e^{y_1 - y_2})^{-1} dy_2 \quad (\text{A-8})$$

and the y_2 integration can be carried out in an analogous manner as that of y_3 to obtain

$$- (1 + e^{y_1})^{-1} (3\xi(2) + \frac{1}{2}y_1^2), \quad (\text{A-9})$$

where $\xi(2) = \pi^2/6$ is the Riemann zeta function. Now,

$$I(\Delta) = \int_{-\Delta}^{\infty} [(y + \delta)^2 - \beta^2 m_4^2]^{1/2} (3\xi(2) + \frac{1}{2}y^2) \\ \times (1 + e^y)^{-1} (1 + e^{-(y + \Delta)})^{-2} dy \quad (\text{A-10})$$

and

$$\{I(\Delta) - I(-\Delta)\} \propto \int_{-\Delta}^{\Delta} \dots \quad (\text{A-11})$$

These equations are evaluated numerically.

Appendix B: F and D Couplings

Here we provide a brief review of some of the results of $SU(3)$, with emphasis on the types of baryon-baryon-meson couplings allowed in an invariant theory. *The Eightfold Way*, Gell-Mann and Ne'eman (1964), is a collection of many reprints of the original papers on $SU(3)$, and provides the background for this discussion. In the construction of the F and D couplings we follow the treatment of Frazer (1966) (a simplified and general discussion, especially comprehensible to those with little background in $SU(3)$).

We use the eight hermitian generators of infinitesimal transformations

$$Q = I + i \sum_{j=1}^8 \lambda_j \Theta_j \quad (\text{B-1})$$

defined by Gell-Mann and Ne'eman (1964) as

$$\begin{aligned} \lambda_1 &= I_+ + I_-, & \lambda_4 &= V_+ + V_-, & \lambda_6 &= U_+ + U_-, \\ \lambda_2 &= iI_- - iI_+, & \lambda_5 &= iV_+ - iV_-, & \lambda_7 &= iU_- - iU_+, \\ \lambda_3 &= 2I_3, & \lambda_8 &= \frac{2}{\sqrt{3}}(U_3 - V_3), \end{aligned} \quad (\text{B-2})$$

where the I 's, U 's and V 's are a set of 3×3 matrices, which act as raising and lowering operators analogous to I spin in $SU(2)$. The I_3 , U_3 and V_3 commute and their eigenvalues can be used to label states. For reference we write down these eight 3×3 matrices from Gell-Mann and Ne'eman (1964) as

$$\begin{aligned} \lambda_1 &= \begin{pmatrix} 0 & 1 & 0 \\ 1 & 0 & 0 \\ 0 & 0 & 0 \end{pmatrix}, & \lambda_2 &= \begin{pmatrix} i & -i & 0 \\ i & 0 & 0 \\ 0 & 0 & 0 \end{pmatrix}, \\ \lambda_3 &= \begin{pmatrix} 1 & 0 & 0 \\ 0 & -1 & 0 \\ 0 & 0 & 0 \end{pmatrix}, & \lambda_4 &= \begin{pmatrix} 0 & 0 & 1 \\ 0 & 0 & 0 \\ 1 & 0 & 0 \end{pmatrix}, \\ \lambda_5 &= \begin{pmatrix} 0 & 0 & -i \\ 0 & 0 & 0 \\ i & 0 & 0 \end{pmatrix}, & \lambda_6 &= \begin{pmatrix} 0 & 0 & 0 \\ 0 & 0 & 1 \\ 0 & 1 & 0 \end{pmatrix}, \\ \lambda_7 &= \begin{pmatrix} 0 & 0 & 0 \\ 0 & 0 & -i \\ 0 & i & 0 \end{pmatrix}, & \lambda_8 &= \begin{pmatrix} \frac{1}{\sqrt{3}} & 0 & 0 \\ 0 & \frac{1}{\sqrt{3}} & 0 \\ 0 & 0 & -\frac{2}{\sqrt{3}} \end{pmatrix}. \end{aligned} \tag{B-3}$$

The simplest extension of $SU(2)$ is to form a triplet \mathbf{q} from the three unit vectors

$$q^1 = \begin{pmatrix} 1 \\ 0 \\ 0 \end{pmatrix}, \quad q^2 = \begin{pmatrix} 0 \\ 1 \\ 0 \end{pmatrix}, \quad q^3 = \begin{pmatrix} 0 \\ 0 \\ 1 \end{pmatrix}, \tag{B-4}$$

and an arbitrary vector \mathbf{q} can be written in terms of the three unit vectors. If we now represent states in terms of the eigenvalues $|I_3, U_3, V_3\rangle$ we have, (applying the operators (B-3) to (B-4)),

$$\mathbf{q}^1 = |\frac{1}{2}, 0, -\frac{1}{2}\rangle, \quad \mathbf{q}^2 = |-\frac{1}{2}, \frac{1}{2}, 0\rangle, \quad \mathbf{q}^3 = |0, -\frac{1}{2}, \frac{1}{2}\rangle, \tag{B-5}$$

and the q^i transform as

$$q'^i = Q_{ij} q^j. \tag{B-6}$$

In $SU(3)$ there exists another set of vectors in the triplet representation which are complex to q_i and are labeled \bar{q}_i . If we take the complex conjugate of Equation (B-6), we have

$$\bar{q}'_i = Q_{ij}^* \bar{q}_j \tag{B-7}$$

and the \bar{q} transforms according to Q^* as

$$Q^* = I + i \sum_1^8 \bar{\lambda}_i \Theta_i \tag{B-8}$$

and

$$\bar{\lambda}_i = -\lambda_i^* \quad (\text{B-9})$$

From the matrices in (B-3) we find

$$\bar{I}_3 = -I_3, \quad \bar{U}_3 = -U_3, \quad \bar{V}_3 = -V_3, \quad (\text{B-10})$$

so that

$$\bar{\mathbf{q}}_1 = |-\frac{1}{2}, 0, \frac{1}{2}\rangle, \quad \bar{\mathbf{q}}_2 = |\frac{1}{2}, -\frac{1}{2}, 0\rangle, \quad \bar{\mathbf{q}}_3 = |0, \frac{1}{2}, -\frac{1}{2}\rangle. \quad (\text{B-11})$$

We can now use the q and \bar{q} to form multiplets, such as

$$q^i \bar{q}_i \quad \text{a singlet (0)} \quad (\text{B-12})$$

$$T_j^i = q^i \bar{q}_j - \frac{1}{3} \delta_j^i q^k \bar{q}_k \quad \text{an octet (8)}. \quad (\text{B-13})$$

In Equation (B-13) T has nine terms, but since its trace is zero only eight are independent. Gell-Mann and Ne'eman (1964) made the first successful assignments of the baryons and mesons to the T_j^i octet. Their results are summarized in Table III (taken from Frazer, 1966)

TABLE III

State	I_3	U_3	V_3	B	M
T_2^1	1	$-\frac{1}{2}$	$-\frac{1}{2}$	Σ^+	π^+
T_1^2	-1	$\frac{1}{2}$	$\frac{1}{2}$	Σ^-	π^-
T_3^1	$\frac{1}{2}$	$\frac{1}{2}$	-1	P	K^+
T_1^3	$-\frac{1}{2}$	$\frac{1}{2}$	-1	\bar{E}^-	K^-
T_3^2	$-\frac{1}{2}$	1	$-\frac{1}{2}$	N	K^0
T_2^3	$\frac{1}{2}$	-1	$\frac{1}{2}$	\bar{E}^0	\bar{K}^0
T_1^1	0	0	0	$\frac{\Sigma^0}{\sqrt{2}} + \frac{A^0}{\sqrt{6}}$	$\frac{\pi^0}{\sqrt{2}} + \frac{\eta}{\sqrt{6}}$
T_2^2	0	0	0	$\frac{-\Sigma^0}{\sqrt{2}} + \frac{A^0}{\sqrt{6}}$	$\frac{-\pi^0}{\sqrt{2}} + \frac{\eta}{\sqrt{6}}$
T_3^3	0	0	0	$-\sqrt{\frac{2}{3}} A^0$	$-\sqrt{\frac{2}{3}} \eta$

T_j^i matrix

Under $SU(2)$ one assumed that for nucleons the $NN\pi$ interaction should be invariant in I spin space. This assumption implies a coupling of the form $N_f^+ \tau N_i \cdot \pi$, which has had much success in predicting branching ratios. For the baryon-baryon-meson coupling in $SU(3)$ one performs an analogous operation and forms invariants from the matrices representing the octets. Our notation is such that P is a destruction operator for a proton and a creation operator for an antiproton, while \bar{P} is the reverse of this. In $SU(3)$ there are two ways to write an invariant coupling, $\text{Tr}(\bar{B}BM)$ and $\text{Tr}(B\bar{B}M)$; as the trace is invariant under cyclic permutations all other invariants can be transformed into these two. By convention one considers linear combinations of these invariants and labels them as

$$D \text{ type: } \text{Tr}[(B\bar{B} + \bar{B}B)M] \quad (\text{B-14})$$

$$F \text{ type: } \text{Tr}[(B\bar{B} - \bar{B}B)M] \quad (\text{B-15})$$

which can be written out (Frazer, 1966) as

D type

$$\begin{aligned} &= \frac{1}{\sqrt{2}} \pi^0 (\bar{P}P - \bar{N}N + \frac{2}{\sqrt{3}} \bar{\Sigma}^0 \Lambda + \frac{2}{\sqrt{3}} \bar{\Lambda} \Sigma^0 - \bar{\Xi}^0 \Xi^0 + \bar{\Xi}^- \Xi^-) \\ &+ \frac{1}{\sqrt{6}} \eta (-\bar{P}P - \bar{N}N - 2\bar{\Lambda} \Lambda + 2\bar{\Sigma}^- \Sigma^- + 2\bar{\Sigma}^+ \Sigma^+ \\ &+ 2\bar{\Sigma}^0 \Sigma^0 - \bar{\Xi}^- \Xi^- - \bar{\Xi}^0 \Xi^0) \\ &+ \pi^+ (\bar{P}N + \bar{\Xi}^0 \Xi^- + \sqrt{\frac{2}{3}} \bar{\Lambda} \Sigma^- + \sqrt{\frac{2}{3}} \bar{\Sigma}^+ \Lambda) \\ &+ \pi^- (\bar{N}P + \bar{\Xi}^- \Xi^0 + \sqrt{\frac{2}{3}} \bar{\Sigma}^- \Lambda + \sqrt{\frac{2}{3}} \bar{\Lambda} \Sigma^+) \\ &+ K^+ \left(-\frac{1}{\sqrt{6}} \bar{P} \Lambda + \frac{1}{\sqrt{2}} \bar{P} \Sigma^0 + \bar{N} \Sigma^- - \frac{1}{\sqrt{6}} \bar{\Lambda} \Xi^- + \frac{1}{\sqrt{2}} \bar{\Sigma}^0 \Xi^- + \bar{\Sigma}^+ \Xi^0 \right) \\ &+ K^- \left(-\frac{1}{\sqrt{6}} \bar{\Lambda} P + \frac{1}{\sqrt{2}} \bar{\Sigma}^0 P + \bar{\Sigma}^- N - \frac{1}{\sqrt{6}} \bar{\Xi}^- \Lambda + \frac{1}{\sqrt{2}} \bar{\Xi}^- \Sigma^0 + \bar{\Xi}^0 \Sigma^+ \right) \\ &+ K^0 \left(\bar{P} \Sigma^+ + \bar{\Sigma}^- \Xi^- - \sqrt{\frac{1}{2}} \bar{N} \Sigma^0 - \frac{1}{\sqrt{6}} \bar{N} \Lambda - \frac{1}{\sqrt{2}} \bar{\Sigma}^0 \Xi^0 - \frac{1}{\sqrt{6}} \bar{\Lambda} \Xi^0 \right) \\ &+ \bar{K}^0 \left(\bar{\Sigma}^+ P + \bar{\Xi}^- \Sigma^- - \frac{1}{\sqrt{2}} \bar{\Sigma}^0 N - \frac{1}{\sqrt{6}} \bar{\Lambda} N - \frac{1}{\sqrt{2}} \bar{\Xi}^0 \Sigma^0 - \frac{1}{\sqrt{6}} \bar{\Xi}^0 \Lambda \right), \end{aligned} \quad (\text{B-16})$$

F Type

$$\begin{aligned} &= \frac{1}{\sqrt{2}} \pi^0 (\bar{P}P - \bar{N}N + 2\bar{\Sigma}^+ \Sigma^+ - 2\bar{\Sigma}^- \Sigma^- + \bar{\Xi}^0 \Xi^0 - \bar{\Xi}^- \Xi^-) \\ &+ \sqrt{\frac{3}{2}} \eta (\bar{P}P + \bar{N}N - \bar{\Xi}^- \Xi^- - \bar{\Xi}^0 \Xi^0) \\ &+ \pi^+ (\bar{P}N - \bar{\Xi}^0 \Xi^- + \sqrt{2} \bar{\Sigma}^0 \Sigma^- - \sqrt{2} \bar{\Sigma}^+ \Sigma^0) \\ &+ \pi^- (\bar{N}P - \bar{\Xi}^- \Xi^0 + \sqrt{2} \bar{\Sigma}^- \Sigma^0 - \sqrt{2} \bar{\Sigma}^0 \Sigma^+) \\ &+ K^+ \left(\frac{1}{\sqrt{2}} \bar{\Sigma}^0 \Xi^- + \sqrt{\frac{3}{2}} \bar{\Lambda} \Xi^- + \bar{\Sigma}^+ \Xi^0 - \sqrt{\frac{3}{2}} \bar{P} \Lambda - \sqrt{\frac{1}{2}} \bar{P} \Sigma^0 - \bar{N} \Sigma^- \right) \\ &+ K^- \left(\frac{1}{\sqrt{2}} \bar{\Xi}^- \Sigma^0 + \sqrt{\frac{3}{2}} \bar{\Xi}^- \Lambda + \bar{\Xi}^0 \Sigma^+ - \sqrt{\frac{3}{2}} \bar{\Lambda} P - \sqrt{\frac{1}{2}} \bar{\Sigma}^0 P - \bar{\Sigma}^- N \right) \\ &+ K^0 (\bar{\Sigma}^- \Xi^- - \sqrt{\frac{1}{2}} \bar{\Sigma}^0 \Xi^0 + \sqrt{\frac{3}{2}} \bar{\Lambda} \Xi^0 - \sqrt{\frac{3}{2}} \bar{N} \Lambda - \bar{P} \Sigma^+ + \sqrt{\frac{1}{2}} \bar{N} \Sigma^0) \\ &+ \bar{K}^0 (\bar{\Xi}^- \Sigma^- - \sqrt{\frac{1}{2}} \bar{\Xi}^0 \Sigma^0 + \sqrt{\frac{3}{2}} \bar{\Xi}^0 \Lambda - \sqrt{\frac{3}{2}} \bar{\Lambda} N - \bar{\Sigma}^+ P + \sqrt{\frac{1}{2}} \bar{\Sigma}^0 N). \end{aligned} \quad (\text{B-17})$$

It is these *F* and *D* couplings which are used in constructing the weak hadronic currents in Section 2.

Appendix C: Evaluating $|M|^2$ for Σ^- Reaction

From Equation (60), we have

$$|M|^2 = \frac{G^2}{2} |F(q^2)|^2 \sin^2 \Theta \cos^2 \Theta \frac{1}{2} \sum_{\substack{S_i \\ S_f}} \bar{u}_p \gamma_\lambda (1 - r\gamma_5) u_n \\ \times \bar{u}_s - \gamma^\lambda (1 - s\gamma_5) u_n \bar{u}_n \gamma^\mu (1 - s\gamma_5) u_s - \bar{u}_n \gamma_\mu (1 - r\gamma_5) u_p. \quad (\text{C-1})$$

Now

$$\Sigma u \bar{u} = \frac{(-i\not{P} + m)}{2m} \quad (\text{C-2})$$

represents the positive energy projection operator (note $P \cdot P = -m^2$), where $u \bar{u}$ have been normalized to unity. Using the subscripts 1 and 2 for the neutrons, 3 for the proton and 4 for the Σ^- , then successive application of the projection operators leads to the following trace form

$$|M|^2 = \frac{G^2}{4} |F(q^2)|^2 \sin^2 \Theta \cos^2 \Theta \text{Tr} \left[\gamma_\lambda (1 - r\gamma_5) \right. \\ \times \left. \frac{(-i\not{P}_1 + m_1)}{2m_1} \gamma_\mu (1 - r\gamma_5) \frac{(-i\not{P}_3 + m_3)}{2m_3} \right] \text{Tr} \left[\gamma^\lambda (1 - s\gamma_5) \right. \\ \times \left. \frac{(-i\not{P}_2 + m_2)}{2m_2} \gamma^\mu (1 - s\gamma_5) \frac{(-i\not{P}_4 + m_4)}{2m_4} \right]. \quad (\text{C-3})$$

Using the trace theorems (Bjorken and Drell, 1965) we get

$$|M|^2 = \frac{G^2}{64} |F(q^2)|^2 \sin^2 \Theta \cos^2 \Theta \prod_{i=1}^4 \frac{1}{m_i} \text{Tr} \left[-(1 + r^2) \gamma_\lambda \right. \\ \times \not{P}_1 \gamma_\mu \not{P}_3 + (1 - r^2) m_1 m_3 \gamma_\lambda \gamma_\mu - 2r\gamma_\lambda \not{P}_1 \gamma_\mu \not{P}_3 \gamma_5 \\ \left. \times \text{Tr} \left[-(1 + s^2) \gamma^\lambda \not{P}_2 \gamma^\mu \not{P}_4 + (1 - s^2) m_2 m_4 \gamma^\lambda \gamma^\mu - 2s\gamma^\lambda \not{P}_2 \gamma^\mu \not{P}_4 \gamma_5 \right] \right]. \quad (\text{C-4})$$

In multiplying the traces we need only retain products symmetric in the P variables, therefore Equation (C-4) becomes,

$$|M|^2 = \frac{G^2}{64} |F(q^2)|^2 \sin^2 \Theta \cos^2 \Theta \prod_{i=1}^4 \frac{1}{m_i} \left[(1 + r^2)(1 + s^2) \right. \\ \times \text{Tr} \gamma_\lambda \not{P}_1 \gamma_\mu \not{P}_3 \text{Tr} \gamma^\lambda \not{P}_2 \gamma^\mu \not{P}_4 \\ - (1 + r^2)(1 - s^2) m_2 m_4 \text{Tr} \gamma_\lambda \not{P}_1 \gamma_\mu \not{P}_3 \text{Tr} \gamma^\lambda \gamma^\mu \\ - (1 - r^2) m_1 m_3 (1 + s^2) \text{Tr} \gamma_\lambda \gamma_\mu \text{Tr} \gamma^\lambda \not{P}_2 \gamma^\mu \not{P}_4 \\ + (1 - r^2) m_1 m_3 (1 - s^2) m_2 m_4 \text{Tr} \gamma_\lambda \gamma_\mu \text{Tr} \gamma^\lambda \gamma^\mu \\ \left. + 4rs \text{Tr} \gamma_\lambda \not{P}_1 \gamma_\mu \not{P}_3 \gamma_5 \text{Tr} \gamma^\lambda \not{P}_2 \gamma^\mu \not{P}_4 \gamma_5 \right]. \quad (\text{C-5})$$

Now

$$\text{Tr} \gamma_\lambda \not{P}_1 \gamma_\mu \not{P}_3 \text{Tr} \gamma^\lambda \not{P}_2 \gamma^\mu \not{P}_4 = 32 [P_1 \cdot P_2 P_3 \cdot P_4 + P_1 \cdot P_4 P_2 \cdot P_3] \quad (\text{C-6})$$

and

$$\text{Tr } \gamma_\lambda \not{P}_1 \gamma_\mu \not{P}_3 \gamma_5 \text{Tr } \gamma^\lambda \not{P}_2 \gamma^\mu \not{P}_4 \gamma_5 = 32 [P_1 \cdot P_2 P_3 \cdot P_4 - P_1 \cdot P_4 P_2 \cdot P_3], \quad (\text{C-7})$$

$$\text{Tr } \gamma^\lambda \gamma^\mu = 4g^{\lambda\mu}. \quad (\text{C-8})$$

Therefore,

$$\text{Tr } \gamma^\lambda \gamma^\mu \text{Tr } \gamma_\lambda \not{P}_1 \gamma_\mu \not{P}_3 = 16P_1 \cdot P_3. \quad (\text{C-9})$$

Finally

$$\begin{aligned} |M|^2 = & \frac{G^2}{4} |F(q^2)|^2 \sin^2 \Theta \cos^2 \Theta \prod_{i=1}^4 \frac{1}{m_i} [2(1+r^2) \\ & \times (1+s^2) [P_1 \cdot P_2 P_3 \cdot P_4 + P_1 \cdot P_4 P_2 \cdot P_3] \\ & + 8rs [P_1 \cdot P_2 P_3 \cdot P_4 - P_1 \cdot P_4 P_2 \cdot P_3] \\ & + 4 \prod_{i=1}^4 m_i (1-r^2) (1-s^2) + m_2 m_4 (1+r^2) (1-s^2) P_1 \cdot P_3 \\ & + m_1 m_3 (1-r^2) (1+s^2) P_2 \cdot P_4]. \end{aligned} \quad (\text{C-10})$$

Acknowledgements

This work was submitted by one of us (W.L.) in partial fulfillment of the requirements for a Ph.D. at Yale University.

This research was supported in part by grants from the National Science Foundation, the National Aeronautics and Space Administration and the U.S. Atomic Energy Commission.

One of us (W.L.) currently a recipient of a NAS-NRC postdoctoral research associateship, would like to thank Yale University for financial support and Dr. R. Jastrow for his hospitality at the Goddard Institute for Space Studies.

References

- Ambartsumyan, V. A. and Saakyan, G. S.: 1960, *Astron. J. USSR* **37**, 193; 1960, *Soviet Astron. AJ* **4**, 187.
 Arnett, W. D.: 1966, Thesis, Yale University, New Haven, Conn.
 Bahcall, J. N. and Wolf, R. A.: 1965a, b, *Phys. Rev.* **140**, B1452.
 Bjorken, J. and Drell, S.: 1964, *Relativistic Quantum Mechanics*, McGraw-Hill Book Co., New York.
 Brene, N., Hellesen, B., and Roos, M.: 1964, *Phys. Letters* **11**, 344.
 Cabibbo, N.: 1963, *Phys. Rev. Letters* **10**, 531.
 Cameron, A. G. W.: 1959, *Astrophys. J.* **130**, 884.
 Cameron, A. G. W.: 1965, *Nature* **205**, 787.
 Chandrasekhar, S.: 1939, *An Introduction to the Study of Stellar Structure*, Dover Publ. Inc.
 Colleraine, A. P.: 1966, Thesis, Princeton University, Princeton, New Jersey.
 Feynman, R. and Gell-Mann, M.: 1958, *Phys. Rev.* **109**, 193.
 Frazer, W.: 1966, *Elementary Particles*, Prentice Hall, New Jersey.
 Gell-Mann, M. and Ne'eman, Y.: 1964, *The Eightfold Way*, W. A. Benjamin, Inc., New York, N.Y.
 Gershtein, S. S. and Zeldovich, J. B.: 1955, *JETP* **2**, 576.
 Hansen, C. J.: 1966, Thesis, Yale University, New Haven, Conn.

- Hansen, C. J. and Tsuruta, S.: 1967, *Can. J. Phys.* **45**, 2823.
Jackson, J. D. and Pilkuhn, H.: 1964, *Nuovo Cimento* **33**, 906. Errata, *Nuovo Cimento* **34**, 1841.
Levinger, J. S. and Simmons, L. M.: 1961, *Phys. Rev.* **124**, 916.
Rosenfeld, A. H., Barbaro-Galtieri, A., Padolsky, W. J., Price, L. R., Roos, M., Soding, P., Willis, W. J., and Wohl, C. G.: 1967, *Rev. Mod. Phys.* **39**, 1.
Selleri, F.: 1961, *Phys. Rev. Letters* **6**, 64.
Tsuruta, S.: 1964, Thesis, Columbia University, New York, N.Y.
Tsuruta, S. and Cameron, A. G. W.: 1966, *Can. J. Phys.* **44**, 1895.
Wolf, R.: 1966, *Astrophys. J.* **145**, 834.
Wu, C. S.: 1964, *Rev. Mod. Phys.* **36**, 2, 618.